

Chapter 2

The Role of Metrics in Performance-Based Design

2.1 Introduction

To evaluate the performance of buildings in use and to predict performance during design, it is necessary to identify what the appropriate measures of performance should be, when and how measures should be collected, and how results will be interpreted to determine success or failure. As noted in Chap. 1, one of the central barriers to effective daylighting is that daylighting *performance* is often defined differently by different stakeholders, leading to a fragmented approach to performance assessment in the design and operational life-cycle of buildings. While daylighting has most consistently been promoted as a means of electrical lighting energy reduction, greater understanding of the health benefits of daylight and views combined with greater awareness of discomfort glare and the mandate to minimize heating/cooling loads to achieve low and Zero Net Energy (ZNE) buildings has led to an expanding set of performance considerations. Existing metrics, performance criteria and methodologies for assessing daylit spaces have evolved largely from the legacy of metrics developed for the electrical lighting industry, and hold many of the same underlying assumptions. Therefore, it is important to identify and understand the strengths, weaknesses and limitations of these assumptions in assessing the dynamic qualities of daylight spaces.

There are many indicators available for design teams to predict and assess the outcome of daylighting strategies, each with underlying assumptions for the lighting needs, preferences and behaviors of building occupants. This chapter presents a broad assessment of the energy and human-factors performance metrics that should be considered to achieve effectively daylit buildings. The chapter is divided into sections, each discussing a key performance objective. The chapter prioritizes discussion of metrics implemented in consensus-based green building rating systems, whole-building energy benchmarking frameworks and targets, and in software-based evaluation tools on the basis that these metrics are anticipated to have the greatest short-term influence on the design and evaluation of daylit buildings.

Discussion of each performance objective concludes with an assessment of the limitations with existing approaches and potential opportunities for improvement.

2.2 Optimizing Energy in High-Performance Daylit Buildings

A number of energy efficiency and GHG reduction goals have been developed to transform the design and operation of buildings into an effective tool for mitigating climate change. In the United States, the most ambitious effort is the State of California Long-Term Energy Efficiency Strategic Plan, which has developed and is now striving to implement a vision for all new commercial construction to be Zero Net Energy (ZNE) by 2030 and for 50% of existing commercial buildings to be retrofit to achieve deep levels of energy reduction to achieve ZNE with the addition of clean distributed power generation (CPUC 2008). California also has even more challenging carbon goals to achieve by 2050. A ZNE building is generally defined as, “an energy-efficient building where, on a source energy basis, the actual annual delivered energy is less than or equal to the on-site renewable exported energy” (U.S. DOE 2015). A critical assessment of various ZNE definitions can be found in (Torcellini et al. 2006). While the intent of ZNE is good, we note that in dense urban areas with high rise commercial buildings incorporating energy intensive functions, e.g. data centers, hospitals, etc. it may be physically impossible to meet the requirement with on-site renewables alone.

The emergence of low and ZNE performance goals (discussed in Chap. 1) has placed effective daylighting at the core of whole-building energy efficient design. In commercial buildings, which account for roughly half of the energy used by all U.S. buildings, decisions related to fenestration affect the majority of energy end uses and are thus a central area of focus for performance improvements aimed at enabling low and ZNE buildings. While there are numerous variations on the definition of ZNE, Fig. 2.1 illustrates the general concept. Zero Net Energy is often assessed using the metric of Energy Use Intensity (EUI), which is typically calculated by dividing the total site (or source) energy consumed by the building in one year (measured in kBtu, GJ, or kWh) by the total gross floor area of the building (measured in ft² or m²).

The transmission of daylight through windows (i.e. sidelighting) as a strategy for energy reduction is based on a simple concept: daylight is a renewable light source of high luminous efficacy, which makes the daylighting of buildings an attractive energy strategy compared to the standard practice of constant electrical lighting. As noted in Chap. 1, in the United States, lighting represents the single largest commercial building electricity end use (0.78 exajoules (EJ)) (724 Trillion Btu) (EIA 2012), and is consumed primarily during daylight hours. Of the total averages, it is estimated that 60% is consumed in perimeter zones¹ located 0–12.2 m (0–40 ft) from the building facade during typical daytime work hours (8:00–18:00) (Shehabi et al. 2013).

¹Excluding non-applicable floor space such as religious worship or vacant space.

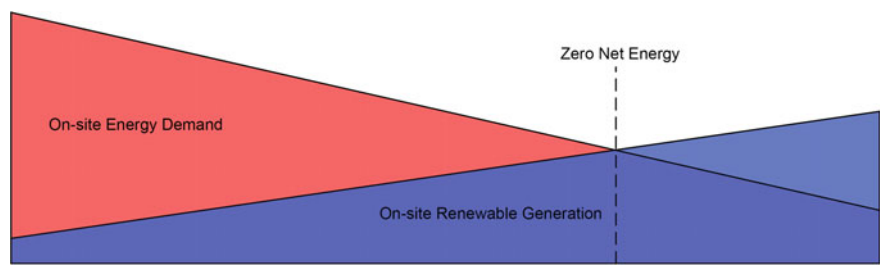


Fig. 2.1 A Zero-Net Energy (ZNE) building generates at least as much energy as it consumes annually

Cooling loads represent another significant energy end use (14%), and one-third is due to electrical lighting and another one-third to solar heat gains through windows (Huang and Franconi 1999). And, because ZNE projects often implement passive or low-energy cooling alternatives such as radiant systems or exposed thermal mass with night-flush ventilation, effective solar control is an additional requirement to avoid exceeding the cooling capacities of these systems, which are typically lower than mechanical HVAC, and consequently more sensitive to peak solar heat gains. Consequently, fenestration strategies that control solar loads and manage glare while transmitting sufficient daylight to minimize the need for electrical lighting in perimeter zones have the potential to significantly improve energy performance.

Figure 2.2 compares the Energy Use Intensity (EUI) of an average office building in Seattle to the recently constructed Bullitt Center (Fig. 2.3), a 6-floor, 4645 m² office building designed to achieve ZNE on an annual basis using electricity generated from a rooftop solar photovoltaic (PV) array (a case study

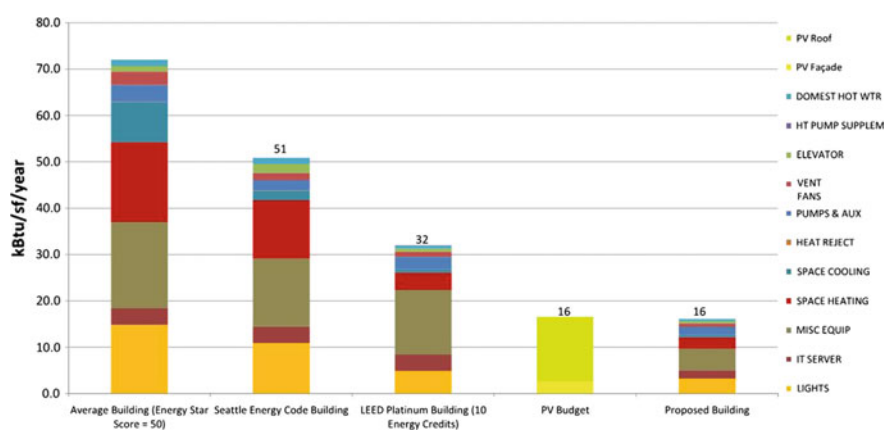


Fig. 2.2 Comparison of the Seattle Bullitt Center (at 50.5 kWh/m²/yr (16 kBtu/ft²/year) with various EUI benchmarks and with the renewable energy available from its own rooftop photovoltaic array. *Image credit* The Miller Hull Partnership



Fig. 2.3 Exterior view of the Bullitt Center showing rooftop solar PV array and exterior automated shading devices

description of the Bullitt Center is provided in Chap. 5). Due to the spatial constraints of the project site, the available area for a PV array on the roof combined with the relatively cloudy Seattle climate led to a renewable energy “budget” of 50.5 kWh/m²/yr (16 kBtu/ft²-yr). Compared with an average Seattle office building, or even a LEED Platinum office building, the PV budget was found to meet only 22 and 50% of those annual energy requirements respectively (Fig. 2.2). Driven by the spatial constraints of the site, local climatic conditions, and the ZNE performance target, the design team worked to develop a highly efficient building envelope to minimize loads and enable the application of passive environmental control strategies of daylighting, direct gain solar heating, natural ventilation, and night-flush cooling. These strategies were combined with low-energy mechanical systems (ground source heat pumps, in-floor radiant heating/cooling, and a Dedicated Outdoor Air System (DOAS) with heat recovery, and resulted in a designed EUI that could be met by the renewable energy budget of 50.5 kWh/m²/yr (16 kBtu/ft²-yr).

Daylighting, a thermally efficient envelope, and actively managed fenestration systems are key components of the Bullitt Center whole-building energy efficiency strategy. Figure 2.2 shows the result of daylighting on electrical lighting EUI, where daylight effectively reduces the operational hours of electrical lighting.

Similarly, automated facade shading acts as a dynamic filter to enable both passive solar heating and solar shading when required to significantly reduce space heating and cooling loads.

2.2.1 From Daylight “Harvesting” to Daylight Autonomous Buildings

While EUI is perhaps the singular most consensus-based metric for gauging energy efficient design, human factors ultimately determine the long-term viability of design strategies, and serve as the underlying basis for differentiating energy “use” from simply energy consumption or waste. Figure 2.4, which presents an interior view of the perimeter zone workspaces within the Bullitt Center, illustrates how a project designed to achieve a low EUI was able to maintain relatively large areas of facade glazing in heating dominated climate, preserving daylight access and views for occupants. In Fig. 2.4, it is important to note the absence of a conventional installation of direct/indirect electrical lighting fixtures on the ceiling. As part of the overall ZNE goal, the client decided to install minimal fixtures and require tenants to install supplemental electrical lighting if desired as a tenant improvement. On site observations revealed that no tenants have installed additional electrical lighting as of the publishing of this book. Because tenants were satisfied with the lighting



Fig. 2.4 Sixth floor daylight perimeter zone. *Note the absence of a conventional installation of electrical lighting fixtures on the ceiling*

conditions provided by daylight, (supplemented with task lighting when necessary), the installed electrical lighting power demand is extremely low, or zero in many spaces.

This outcome is notable, as it indicates that the perimeter zones effectively operate as “daylight autonomous” spaces from the perspective of their occupants. In conventional energy efficient lighting design practices, daylight perimeter zones would be designed with photocontrolled (i.e. daylight-dimming) ambient lighting systems to “harvest” available daylight, rather than be considered as zones that should require no installed ambient lighting. The Bullitt Center provides a glimpse of the potential for perimeter zones to be classified as “daylight autonomous,” where significant energy and cost savings can be achieved through the minimization or elimination of supplemental electrical lighting within 4 or 5 m (13–16.5 ft) from the facade. The critical lesson is that the performance of the architectural daylighting strategy and resulting occupant-based daylight availability should be evaluated prior to the consideration of technology solutions that may reduce energy, but be viewed as unnecessary from the perspective of building occupants.

At any point in time, codes and standards for lighting dictate much of what is designed and built. Practitioners often assume that the current standard practice is somehow optimized, up to date and reflecting immutable norms that persist over time. In fact, “best practice” in design is in flux all the time, although normally changing slowly since change is always a challenge. A lighting design, completed this year, captures and embodies (1) the owners preferences for what they want for their staff or they think the market wants or will accept, (2) mandatory and voluntary codes and ratings constraints, (3) what the design team can reasonably deliver on time and budget with minimal risk, (4) what competing manufacturers can deliver in volume to a job site, (5) what contractors can properly install and commission, (6) operating costs for electricity and (7) what occupants can effectively operate to meet their needs for comfort, health and productivity.

It is not surprising that while there is much diversity in the practice of lighting design, mainstream practice changes slowly. But change does happen and is driven by (1) emerging technology with enhanced, affordable features, e.g. LEDs, sensors, wireless controls, (2) changing demands by owners, e.g. LEED ratings, (3) changing regulatory requirements, e.g. utility demand response programs, stricter state building codes, (4) economic pressures of operating costs, and (5) new knowledge and perspectives about occupant performance, needs and preferences with respect to lighting.

Less than 100 years ago daylight was the preferred and primary source of lighting in many buildings. The advent of the electric light, and particularly the fluorescent lamp, and the growth of an electric infrastructure to deliver power to every building transformed the design of lighting in buildings. Permanent Supplementary Artificial Lighting (PSALI) was the new invention at the time, based on the underlying novel concept that one could rely on electric lighting as the primary light source rather than daylight. This rapidly became the norm for office

design and as the cost of delivered electric lumens fell, office lighting standards suggested uniformly high illuminance levels throughout occupied spaces, and even operating the lights 24 hours a day to provide heating. In an era when low and high pressure lamps were improving in output and color, and when nuclear power promised electricity that would be “too cheap to meter” this vision of building lighting became the norm.

While lamp technology continued to improve, the availability of cheap, reliable energy ended abruptly in the 1970s, first driven by availability, and later by environmental concerns related to carbon emissions. In that context “daylight” was rediscovered as a strategy to reduce reliance on electric lighting by simply reducing output to lights when the resource was available. The design skills of 50 years earlier in terms of how to size and manage fenestration to admit daylight without glare or solar load were rediscovered, reinvented and improved upon, as was the lamp, sensors and controls infrastructure needed to capture the potential savings. But these changes never made it into the mainstream of practice and are just now being mandated by some building codes, the last step in the process of more widespread adoption. We are now 40+ years into that new cycle of change and once again technology, i.e. new efficient light sources and the Internet of Things, is driving some of that change. But major new forces on “best practice” is also being driven by a renewed interest in the role of lighting and daylighting on occupant health, well being, comfort and performance, factors that were often overlooked, forgotten or ignored in the past. In this new context there are exciting changes in play in the design landscape for lighting and daylighting design.

As design goals shift from electrical lighting energy “savings” towards efforts to optimize the potential of daylighting within a whole-building energy concept, reliable performance indicators and methods for assessing daylight sufficiency during design are needed. While assessments of EUI, peak demand, and peak cooling loads are critical for meeting carbon reduction targets, demand side load management, and for enabling the application of low-energy cooling technologies in daylit buildings, emerging metrics for assessing daylight sufficiency are critical for optimizing energy goals around end-user needs and preferences for daylit environments. The following section frames emerging research in Climate Based Daylight Modeling (CBDM) and associated metrics as an effort to improve the ability of designers to deliver daylight autonomous buildings.

2.3 From Static to Dynamic, Climate-Based Daylighting Metrics

As designers seek to go from simply “maximizing” daylight through architectural transparency to thoughtfully managing the admission of daylight to address explicit programmatic and occupant needs within the limits of local climate and building energy goals, new metrics that are sensitive to the unique, time-varying daylighting conditions of the project site and local climate are needed. Historically, the daylight

factor (DF) was the most widely applied metric used to assess daylight sufficiency (Nabil and Mardaljevic 2005). The daylight factor is defined as the ratio of the internal illuminance at a point in a building to the unshaded, external horizontal illuminance under a CIE overcast sky, (Moon and Spencer 1942). It originated in Europe as a metric to assess the daylight conditions needed to provide minimally “adequate” daylight levels. Since the worst case conditions i.e. minimum daylight levels, were overcast skies, that was used as the basis for analysis. Use of the DF method is common because it is simple to understand and relatively easy to measure, leading to its use in codes and standards in the UK and Europe. Over time DF began to be used as a metric to assess annual performance, which it is poorly equipped to do because it does not account for clear skies, partly cloudy conditions or direct sunlight.

The use of DF as a metric to assess daylighting performance has been further compromised because the absolute values selected as design targets have not always been well thought out. In previous versions of LEED, (e.g. USGBC 2009), an average DF of 2% across a given space was required for it to be considered sufficiently daylighted. Since it did not account for direct sun conditions the actual daylight values in spaces could be much higher. In addition because it is based on assessments of horizontal illuminance under standard overcast sky conditions, it is not sensitive to building orientation, geographic location, sun position, or daily/seasonal changes in sky conditions. This is particularly problematic for projects that are located in climates where standard overcast skies rarely exists, and for low and ZNE projects where assessing solar control is a critical design factor. Second, because the DF does not account for the effects of direct beam radiation, and because there is no consensus for an acceptable “upper limit” for the ratio, the DF approach has been criticized for incentivizing a “the more transmission the better” approach, where spaces that would have uncomfortable direct sun or glare can not be differentiated. Finally, the DF approach does not easily allow for the evaluation of aspects of the design that may respond dynamically to changes in weather or sun position, such as automated facade systems or interior shading devices, which are increasingly common in low and ZNE projects.

To address the overly simplified static approach of the DF more complex hourly daylight simulation models were developed beginning in the 1980s. These started with the geometric design of the space to be modeled, utilized the optical properties of glazing and shading systems and calculated the interior daylight levels at several locations in the room using a variety of methods for given latitude, time of year, hour of the day, and weather conditions (Ward 1998). To determine annual energy impacts simplified versions of these models were embedded in hourly simulation programs such as DOE-2, which then calculated daylight levels at several control points in a space on an hour by hour basis using location-specific hourly weather files (Selkowitz et al. 1982). These tools provided hourly illuminance data at control points throughout the year that were climate dependent, location dependent and orientation dependent, and could accommodate the deployment of shading systems, and also calculated simplified glare indices on an hourly basis. These hourly data were primarily used to estimate annual lighting energy savings and overall building energy performance with a focus on the daylighting solution as an energy saving

strategy. Most of the 8760 hourly calculations were completed using coefficient modeling approaches due to the computational intensity of the more accurate first principles calculations and the limitations of the widely used desktop computing systems.

Increased interest in the “subtleties” of daylighting performance coupled with improved models and more computational power now provide more options to determine climate specific data on a more granular spatial and temporal scale. To enable the dynamic, time-varying attributes of a project and its climate to be more fully evaluated, researchers have further developed an approach now generally referred to as Climate Based Daylight Modeling (CBDM) (Mardaljevic 2006). Climate Based Daylight Modeling involves the prediction of interior daylighting conditions over an annual period using sky models derived from standardized hourly weather data representative of the project location. The benefit of CBDM is that it enables designers to develop projects in response to the unique solar and weather conditions of the project site as well as to more readily implement dynamic changes in daylight apertures such as automated facade systems deployed for direct sun control or manually operable interior shading devices deployed to reduce glare. Figure 2.5 presents a comparison of annual hourly weather information (global horizontal illuminance (lux)) between Stockholm, Sweden and Phoenix, Arizona that illustrates differences in the seasonal availability and intensity of daylight. By examining daily and seasonal changes in the spatial patterns and intensity of daylight, designers can predict where and when designs perform well or poorly in regard to daylight sufficiency as well as the potential for glare and solar over-heating. The outcome of a thoughtful design process utilizing CBDM is a unique design solution tuned to the local site. While CBDM provides more site-specific quantitative prediction of daylit illuminances achieved by a particular design option, the approach introduces a number of additional considerations, such as what amounts of daylight are considered insufficient or sufficient by occupants, how dynamic changes in light should be assessed spatially and on an annual basis, and what conditions are likely to be associated with glare and the operation of shading devices. The following section discusses the procedures and metrics used in CBDM and concludes with a discussion of limitations and needs for further research.

Because the lighting conditions in a DF assessment are static, the calculation procedures require only a single, “point-in-time” assessment of points with a space and can be achieved in relatively short time using many computational methods including raytracing programs (e.g. Radiance). In contrast, CBDM is a temporal assessment of lighting conditions over a specified time interval. For example, an annual assessment on an hourly basis (assuming daylight hours from 6:00–18:00) would require 4380 unique assessments. Consequently, CBDM developed along with improvements in computing capacity and changes to software simulation approaches. Due to the significant computational time required by raytracing methods, CBDM utilizes the daylight coefficient approach originally developed by

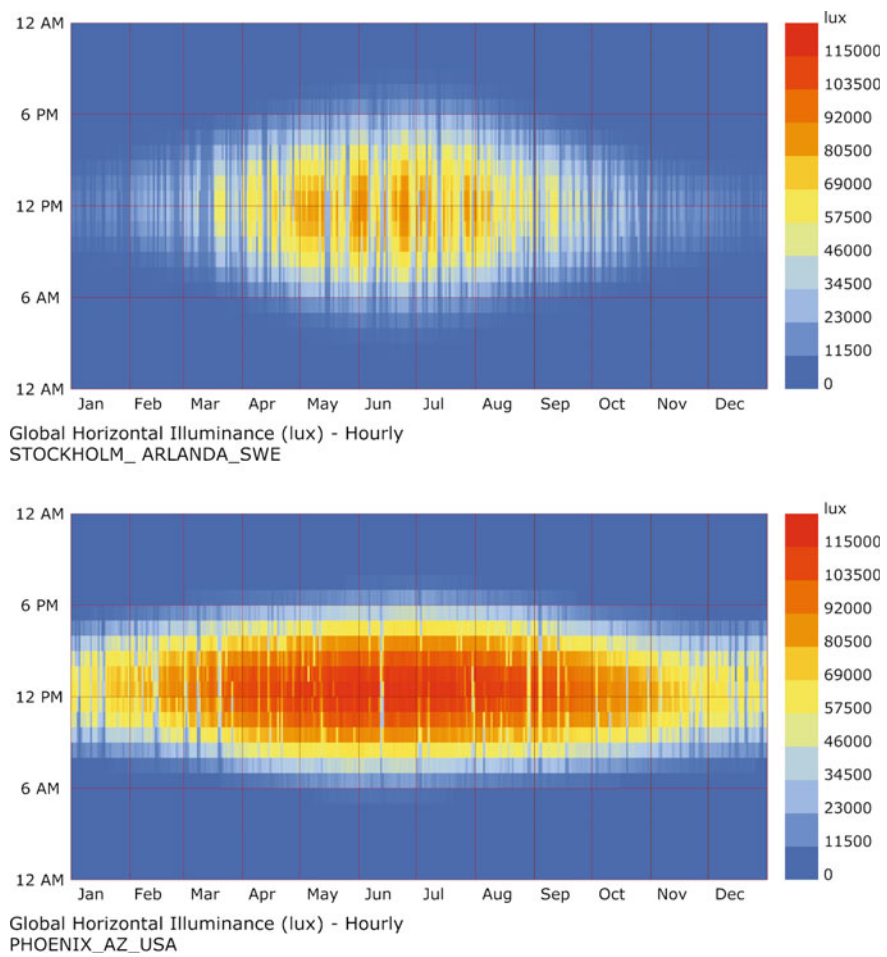


Fig. 2.5 Comparison of availability and intensity of hourly global horizontal illuminances (lux) for Stockholm and Phoenix illustrating differences in the seasonal availability and intensity of daylight between climates

Tregenza and Waters (1983) and first implemented using *Radiance* tools by Reinhart and Herkel (2000) and later standardized by (Bourgeois et al. 2008).

In contrast to conventional raytracing methods, the daylight coefficients for a given point do not depend on the luminance distribution of the sky vault. They are only dependent on the building geometry, aperture dimensions and optical characteristics, interior surface characteristics, and the sub-division of the sky and ground into a matrix of patches (Figs. 2.6 and 2.7). Once the coefficient for each patch has been calculated, an algebraic equation can be used to determine the illuminance at a point, given an arbitrary sky distribution. This approach significantly reduces

Fig. 2.6 Example Tragenza sky matrix consisting of 145 “patches” displayed over a hypothetical sidelit space

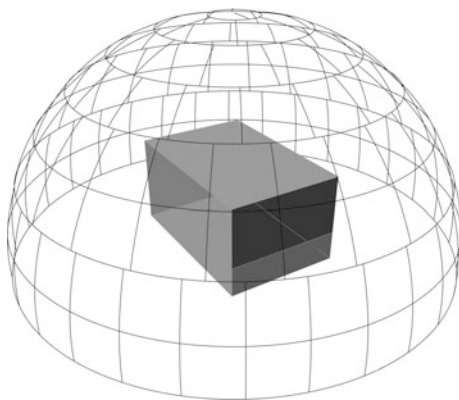
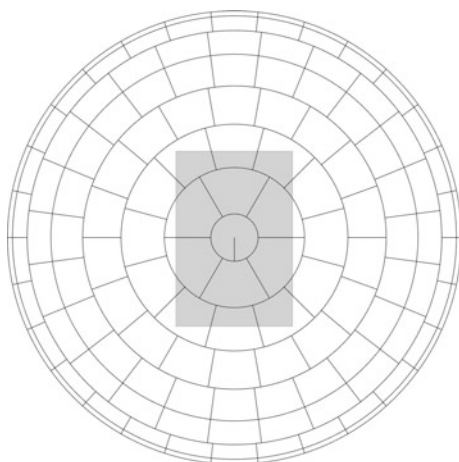


Fig. 2.7 Top view of Tragenza sky matrix



simulation time, enabling the analysis of annual daylighting conditions over short time steps (e.g. hourly). Consequently, the contribution of daily and seasonal changes in daylight availability, direct sun penetration, and glare can be assessed, either cumulatively for the full year, or on an hourly basis while maintaining reasonable photometric accuracy for simple fenestration systems.

2.3.1 Climate-Based Daylighting Performance Metrics

Daylight levels in spaces range over several orders of magnitude i.e. from 10 to 100,000 lx, within a single space over time and weather conditions so metrics that distinguish time dependent effects, upper and lower limits and spatial effects are

all potentially important for design. Several metrics have been proposed to evaluate performance using the CBDM approach. These include *Daylight Autonomy* (DA) (Reinhart 2002), *Useful Daylight Illuminance* (UDI) (Nabil and Mardaljevic 2005), *Continuous Daylight Autonomy* (CDA) (Rogers 2006), and *Spatial Daylight Autonomy* (sDA) (IES 2012). Daylight Autonomy was originally defined by Reinhart as: “The percentage of occupied times of the year when a minimum work plane illuminance threshold of 500 lx can be maintained by daylight alone.” The DA metric is used to indicate the percentage of occupied hours of the year when daylight is sufficient to eliminate the need for electrical lighting. Based on a concern that the binary threshold approach of the original DA criteria artificially differentiated between spaces that may not be perceived as different by the human visual system (e.g. 470 vs. 510 lx), Rogers (2006) proposed the CDA metric, assigns a fractional weighting to illuminances below the established threshold in the annual summary of daylight availability. The original DA criteria were expanded by Nabil and Mardaljevic (2005) in their UDI metric to include a “discomfort” threshold of 2000 lx, and reduced the minimum daylight illuminance threshold to 100 lx. The authors note that these limits are based on reports of occupant preferences and behavior in daylit offices with user-operated shading devices. Occupied hours of the year where the horizontal illuminance does not fall within these limits (100–2000 lx) are omitted from the annual summation of UDI.

The IES Approved Method for sDA and ASE (LM-83) is an attempt to define a standardized calculation and simulation-based modeling methodology to predict daylighting performance. Spatial Daylight Autonomy (sDA) is defined as the percent of an analysis area that meets a minimum horizontal daylight illuminance level (e.g. 300 lx) for a specified fraction (e.g. 50%) of the operating hours per year (IES 2012). It is written using the subscript $sDA_{300,50\%}$. The basis for the illuminance thresholds and performance criteria is largely derived from field research, which consisted of measured data and expert assessments conducted in 61 buildings (Heschong 2012). An sDA outcome is calculated as the percent of analysis points across the analysis area that meet or exceed the 300 lx threshold for at least 50% of the analysis period and is reported a single number ranging from 0 to 100%. The analysis period is from 8:00AM to 6:00PM each day, including weekends, leading to 3650 h per year, regardless of building type, space use (i.e. program), or project location on the earth (e.g. latitude). The IES has defined two performance criteria based on sDA outcomes, “Preferred” and “Nominally Accepted.” Analysis areas must meet or exceed $sDA_{300,50\%}$ over 75% of the analysis points to be rated as “Preferred.” Analysis areas must meet or exceed $sDA_{300,50\%}$ over 55% of the analysis points to be rated as “Nominally Accepted.”

Unlike UDI, sDA has no upper limit on daylight illuminance. Therefore, to evaluate the potential risk of excessive sunlight penetration, the IES daylighting metrics committee developed an accompanying metric entitled Annual Sunlight Exposure (ASE). ASE is a metric that, “describes the potential for visual

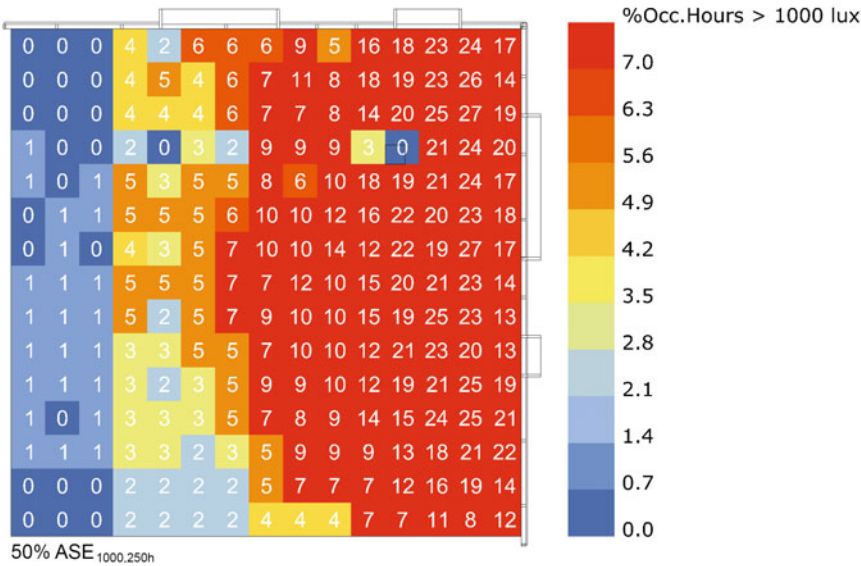
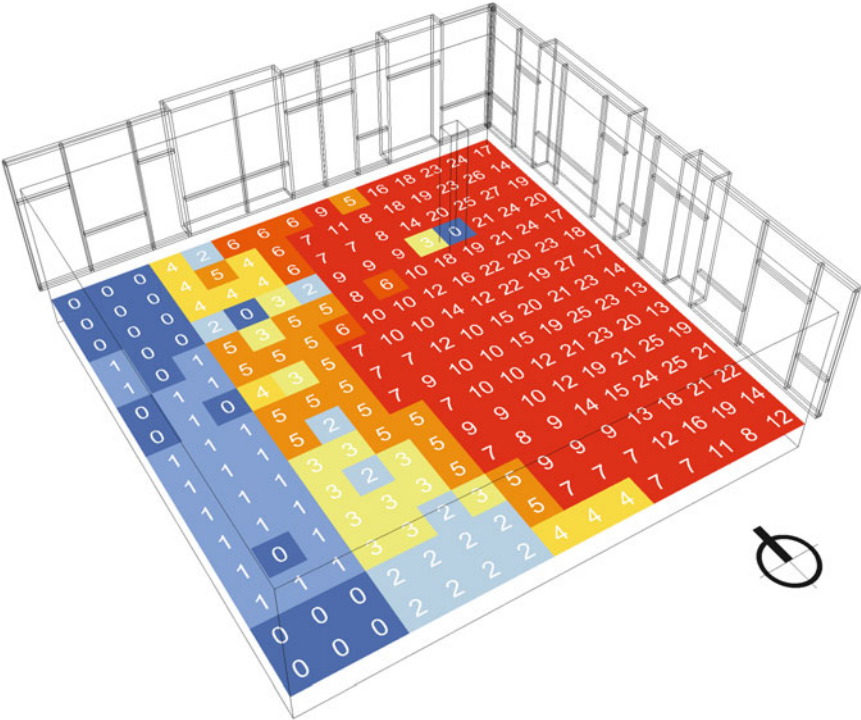
discomfort in interior work environments” (IES 2012). ASE is calculated using the same analysis points and analysis period as sDA and quantifies the percentage of analysis points that receive at least 1000 lx for at least 250 occupied hours per year. It is written using the subscript $ASE_{1000, 250h}$. There are three performance criteria for evaluating excessive sunlight penetration based on $ASE_{1000, 250h}$ outcomes. Daylit spaces predicted to have more than 10% $ASE_{1000, 250h}$ are considered to have “unsatisfactory visual comfort,” spaces with less than 7% are considered “nominally acceptable” and spaces with less than 3% are considered “clearly acceptable” (IES 2012). Notably, the $sDA_{300,50\%}$ ASE simulation method is the first to attempt to standardize the inclusion and operation of interior shading devices to control direct sun in order to present a more realistic prediction of daylight availability in zones considered to have glare and significant periods of direct sun penetration. The simulation method requires that all exterior windows must be modeled with interior shading devices unless the zone associated with the window is determined to be “nominally” or “clearly acceptable” based on $ASE_{1000, 250h}$.

Figure 2.8 presents an example evaluation using $sDA_{300,50\%}$ and $ASE_{1000, 250h}$ of a daylit space with a high level of facade glazing on two elevations. The space is 12 m by 12 m by 3 m in size and the glazed facades are orientated N and E respectively. The project is located in Pasadena, CA (34.15 N latitude), a climate dominated by clear skies and direct sun. Figure 2.8 presents a perspective (upper image) and plan view (lower image) of the $ASE_{1000, 250h}$ analysis. The analysis grid has been enlarged slightly from the recommended maximum spacing (2ft., 0.61 m) to a grid spacing of 0.75 m for illustrative purposes. The $ASE_{1000, 250h}$ analysis shows that the space receives direct sun over a large fraction of the analysis grid and the result of 50% is significantly above the threshold indicating that “unsatisfactory visual comfort” is likely (>10%).

Following the LM-83-12 modeling methodology,² interior window shades and shade operating behavior are included in the calculation of $sDA_{300,50\%}$. Figure 2.9 shows the resulting shading profile for the east-facing window group and Fig. 2.10 shows the shading profile for the north-facing window group. Due to the predominately sunny Pasadena climate, the inclusion of shades which deploy on an hourly basis when more than 2% of analysis points within the window group exceed 1000 lx leads to an east facade that is completely shaded during daylight hours and a north facade that is shaded for a significant number of morning hours.

Figure 2.11 shows the resulting $sDA_{300,50\%}$ outcome for the space. The same grid spacing is used as in Fig. 2.8. As a result of the extensive window shading on the east facade, the region of the space that achieves the greatest levels of DA are oriented towards the north windows, and the contribution of the east facade to interior daylight is minimal, despite the significantly greater amount of solar radiation incident on the facade exterior.

²See IES (2012) for a complete description of the climate modeling methodology.



◀**Fig. 2.8** Perspective view (*upper image*) and plan view (*lower image*) showing ASE_{1000, 250h} result. Each *square* indicates the percentage of occupied hours of the year where the *square* exceeds the illuminance threshold of 1000 lx, a threshold indicator for the presence of direct sun that may cause discomfort. Based on an analysis period of 3650 h per year (10 h per day (8:00AM to 6:00PM) and includes weekends). *Squares in red* indicate regions that exceed 1000 lx for 7% (250 h) or more of the 3650-hour analysis period

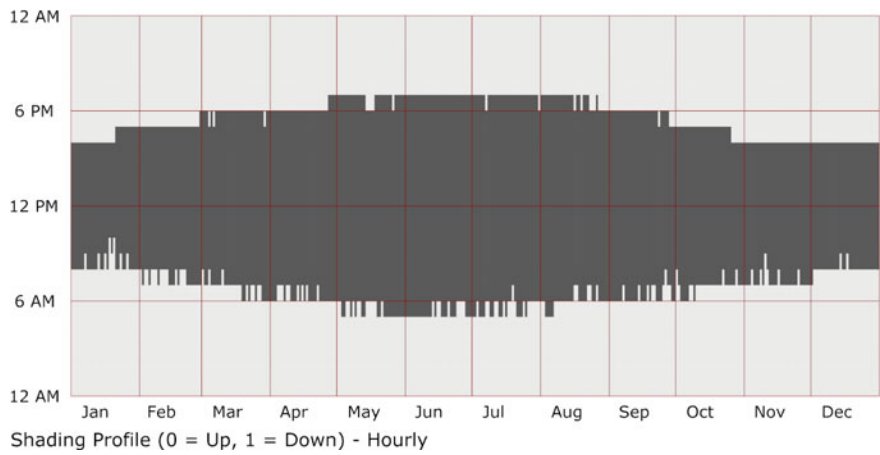


Fig. 2.9 East facade hourly shading profile (*dark grey color indicates shade deployed*)

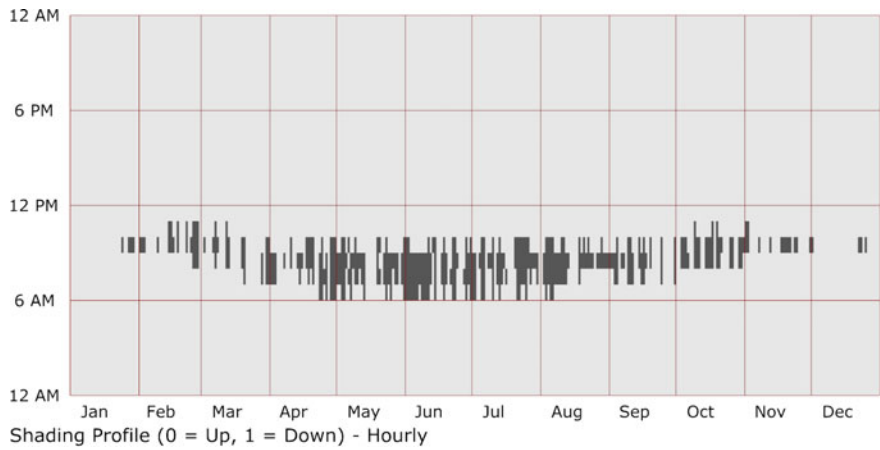


Fig. 2.10 North facade hourly shading profile (*dark grey color indicates shade deployed*)

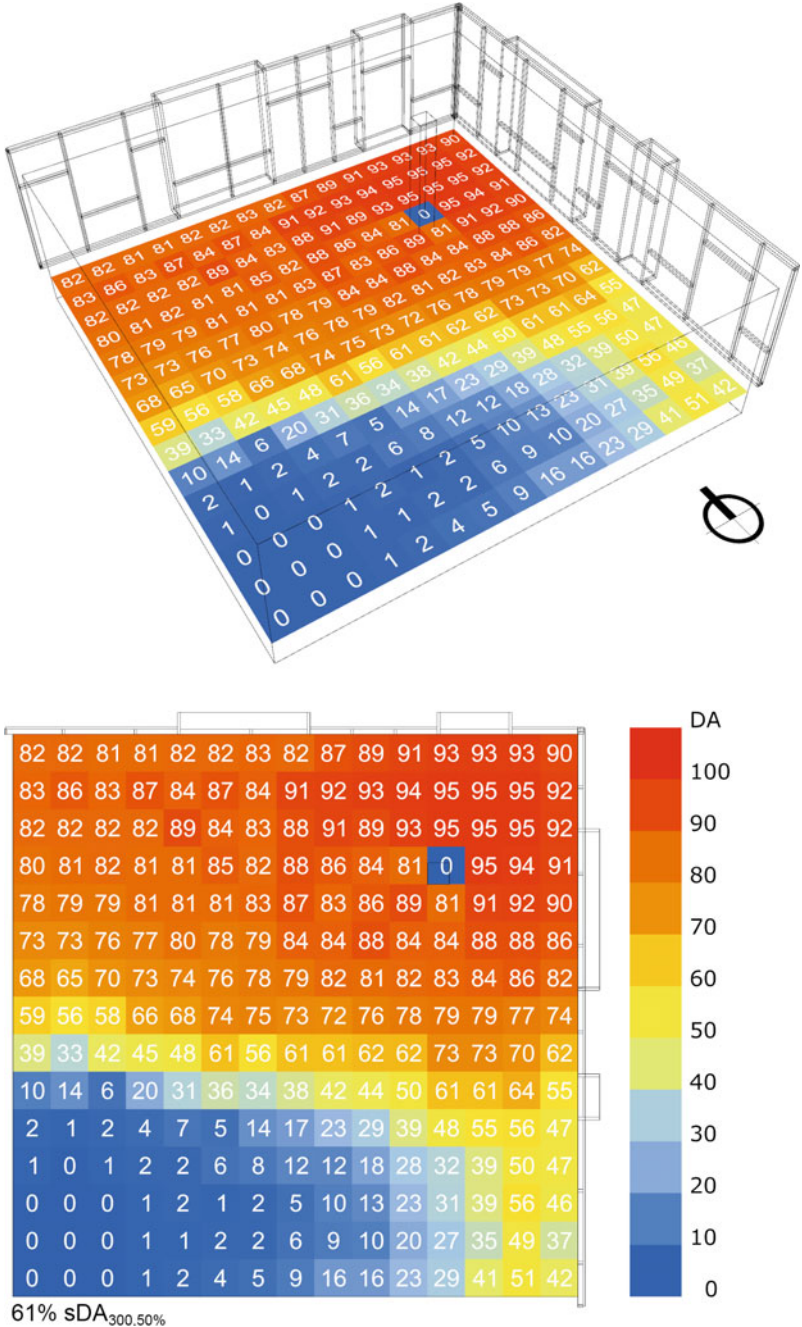


Fig. 2.11 Perspective view (*upper image*) and plan view (*lower image*) showing sDA_{300,50%} result. Each square indicates a unique Daylight Autonomy value, the percentage of occupied hours of the year (0-100%) where the *square* exceeds the illuminance threshold of 300 lx, a threshold indicator for sufficient daylight. The number of *squares* that equal or exceed 50% (138) are divided by the zone total (225) to determine sDA_{300,50%} (138/225 = 61%)

2.3.2 Limitations and Future Directions of Climate-Based Daylight Modeling

Climate Based Daylight Modeling represents significant progress in efforts to improve the fidelity of simulation-based predictions of daylighting performance. In particular, the IES Approved Method for sDA and ASE (LM-83), makes an ambitious effort to link annual daylighting performance of spaces with the preferences and actions of building occupants through assumptions for shading device use. LM-83 has recently been adopted for use in determining compliance with the LEED Daylighting Credit (U.S.G.B.C. 2015). In addition, LM-83 is referenced in ASHRAE 100-2015 (Energy Efficiency in Existing Buildings), and the analysis method used for mandatory and prescriptive photocontrol requirements for California's energy efficiency standard (Title-24) is based on LM-83. Due to the growing use of these systems and standards, one might assume that the IES Approved Method for sDA and ASE will become the consensus metrics used for predictions and claims of effective daylighting. However, it is important to note that very few projects have applied these new metrics and, largely due to the complexity embedded within the annualized simulation methodology, there is no procedure for directly comparing predictions with performance of built projects in use to validate the embedded assumptions regarding occupant needs and behavior. This is perhaps the most significant general limitation of any annualized simulation-based approach to daylighting evaluation.

It is also important to note that these outcomes do not relate directly to energy outcomes for photocontrolled electrical lighting systems. Although Daylight Autonomy is often applied to indicate regions of the work plane where electrical lighting is not required over a period of time, the assumption that either manual switching or dimming, or that a photocontrolled electrical lighting system will modulate light output in direct proportion to incident daylight at each region represents a theoretical upper limit for energy reduction potential. In practice, discrete lighting zones are generally controlled in a closed loop by one interior photosensor placed at a specific point that is intended to be representative of the zone illuminance and having a single view of some region within the zone. Consequently, to simulate lighting energy reduction, at least one sensor point and view vector must be defined for each zone. The modeling of occupant shade control behavior or automated controls adds an additional layer of complexity, due to a similar need to define the critical view points and view vectors for registering the stimulus condition assumed to drive occupant behavior or to control an automated system.

While CBDM methods represent an improvement from assessment methods of the past they are still an evolving work in progress. The following represent factors that should be considered when applying CBDM and some of the new metrics based on IES LM-83 to a design project:

First, the criteria used to differentiate daylight illuminances acceptable to occupants (e.g. 300 lx, global horizontal illuminance) from levels perceived to be insufficient are not supported by a large body of subjective responses to transient daylighting conditions from buildings in use. Rather, the threshold appears to be used largely due to its legacy as a common standard horizontal illuminance level for

electrical lighting design in offices. As visual tasks and office occupancy continue to change these thresholds might change as well.

Second, as suggested by Reinhart (2015), the annual solar exposure limit implemented in LM-83 largely precludes direct sunlight from entering a space, which may be overly restrictive for many space uses where occupants accept (and even prefer) the presence of direct sun. Critical visual tasks in offices may require good control of direct sunlight but there are many workspaces in most building types for which some sunlight penetration may be welcomed, particularly in colder and cloudy climates.

Third, while the human visual system is frequently oriented vertically, sDA and ASE (in addition to all commonly-used daylighting metrics) are derived from measurements of horizontal illuminance on a theoretical “horizontal workplace.” This measurement approach is a legacy of lighting research focused on horizontal visual acuity task performance when workers read documents on a desk and is likely to continue to be poorly applicable to predicting occupant perception and appraisal of the luminous environment with emissive vertical displays in a modern, evolving work space. This is particularly of concern in the assessment of glare. With the eye oriented vertically, direct view of the solar disc or extreme luminance contrasts between windows and indoor surfaces can often become sources of glare and visual discomfort which do not correlate with local (e.g. workstation) measurements of horizontal illuminance.

The fourth limitation is the reliance of daylighting metrics on the photometric quantity of illuminance (lumen per m^2), rather than luminance (candela per m^2). While current daylighting metrics focus exclusively on absolute measurements of illuminance incident on often-imaginary horizontal surfaces, the visual system responds to patterns of luminance in the field of view (the amount of light transmitted, emitted or reflected from real surfaces). Further, the perception of glare in a field of view is known to include an adaptation effect and depends on the luminance of the viewed surface relative to other surfaces in the field of view, not simply the absolute luminance of the surface. Therefore, while measures of horizontal illuminance have a long history in human-factors studies of light, alternative approaches are needed that more closely address the contemporary human experience of light in buildings, both in simulation-based environments and in real buildings. Vertical, luminance-based metrics, such as the assessment of Daylight Glare Probability (DGP) for glare, which leverages the luminance-mapping capabilities of High Dynamic Range (HDR) imaging, present one alternative with significant promise.

Finally, the LM-83 simulation methodology assumes that interior shading devices will be fully deployed by occupants in the presence of direct sun and fully retracted when direct sun is not present. Deviations from this “active operator” assumption in real buildings will result in significantly different quantities of illuminance, which form the basis for the daylight autonomy criteria, as well as differences in glare. To support the effective use of daylighting metrics, it is important to develop a body of human factors data from buildings in use that demonstrates a relationship between the performance indicators and subjective assessments of daylight illuminance. It is additionally important to examine the extent to which

realistic occupant operation or automated operation of shading devices may increase or decrease predicted daylight availability in buildings in use.

2.4 Non-visual Effects of Light

Standards and practices for lighting design (both daylighting and electrical) in buildings were developed based primarily on pragmatic needs of performing visual tasks but only on a limited scientific understanding of the important role light plays in maintaining healthy human biological functions. In indoor environments, where it is estimated that U.S. adults spend nearly 87% of their lives (Klepeis et al. 2001), lighting is often provided by electrical sources that are adequate for visual task performance, but lack the appropriate spectrum and intensity required to stimulate the circadian system. As described by the Illuminating Engineering Society of North America (IESNA), the formal definition of light is “radiant energy that is capable of exciting the human retina and creating a visual sensation” (IESNA 2016). The recent discovery of a third class of photoreceptors in the human retina (Provencio et al. 2000; Gooley et al. 2001; Hannibal et al. 2002; Hattar et al. 2002), referred to as Intrinsically Photoreceptive Retinal Ganglion Cells (ipRGCs), is serving to add an additional and complex set of new considerations and performance expectations for lighting designers.

The human circadian system (or circadian clock) is responsible for orchestrating the daily timing of physical, mental and behavioral changes. These include sleep/wake, alertness level, mood, hormone suppression/ secretion, and core body temperature (CIE 2004). In the majority of humans, the period of the SCN is slightly greater than 24 h. In order to maintain entrainment with the local 24-hour light/dark cycle, the circadian system relies on a resetting response driven by light received at the retina. The magnitude of the resetting response is dependent on a number of parameters including the timing, intensity, duration, wavelength, number and pattern of light exposures (Lockley et al. 2003). The lack of a sufficient light stimulus at the appropriate time can disrupt the circadian system, which can in turn lead to a range of negative health outcomes, such as poor sleep, reduced alertness, and increased risk of a range of health problems including diabetes, obesity, cardiovascular disease and cancer (Zelinski et al. 2014). Common causes of circadian disruption include long-distance travel, night-shift work, exposure to bright light in the evening, and long-term occupancy in poorly lit indoor environments.

Relative to the visual system, which is maximally sensitive to (~ 555 nm) “green” light, the action spectrum of the circadian system is shifted towards shorter wavelength (~ 480 nm) “blue” light (Brainard et al. 2001; Thapan et al. 2001). Thus, the photopic luminous efficacy function (V_{λ}) and standard photometric units (lux) are problematic for assessing the biological effects of various light sources. Figure 2.12 shows the spectral response function of the circadian system (C_{λ}) and the visual system (V_{λ}) along with the Spectral Power Distributions (SPDs) of three CIE daylight illuminants (D55) sunlight, (D65)

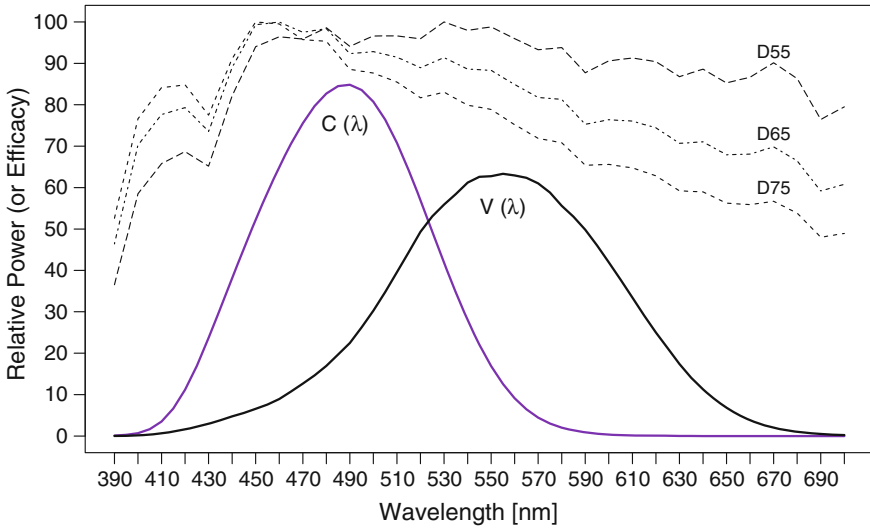


Fig. 2.12 Comparison of spectral response of the visual (photopic) system (V-Lambda) and the circadian system (C-Lambda) to the relative spectral power distributions of three CIE daylight illuminants: (D55) sunlight, (D65) overcast sky, and (D75) north sky daylight. *Note* Both response curves are scaled to have equal area under the curves

overcast sky, and (D75) north sky daylight. It can be seen from Fig. 2.12 that the peak sensitivity of the circadian system (C-lambda) matches closely with the peak power of various daylight SPDs. In contrast, Fig. 2.13 compares the spectral response of the visual system (V-lambda) and the circadian system (C-lambda) to the spectral power distribution a narrow tri-band fluorescent lamp (the CIE illuminant F11) installed in many commercial office building lighting applications. Figure 2.13 shows that the peak power of the fluorescent light aligns closely with the response function of the visual system (V-lambda) and that relatively little power is distributed within the sensitivity of the circadian response function (C-lambda).

Timing of light exposure also plays an important role in synchronizing circadian rhythms with daily patterns of activity (Khalsa et al. 2003). For a typical well-rested and regularly-sleeping individual, a light stimulus in the early morning will advance the circadian clock, causing earlier wake-up time and earlier sleep onset. Alternatively, light received in the evening will delay the circadian clock, causing later wake-up time and later sleep-onset. Light received in the middle of the biological day will have limited effect on circadian advancement or delay, but has been shown to cause reduced levels of sleepiness and higher levels of subjective alertness (Phipps-Nelson et al. 2003; Rüger et al. 2006). Finally, past history of light exposure has an effect on sensitivity of the circadian system to light (Chang et al. 2011). Higher levels of light exposure during the day cause the sensitivity of the circadian system to decrease over time, and lower exposure levels causes sensitivity to increase. A thorough summary of the parameters that control the response of the

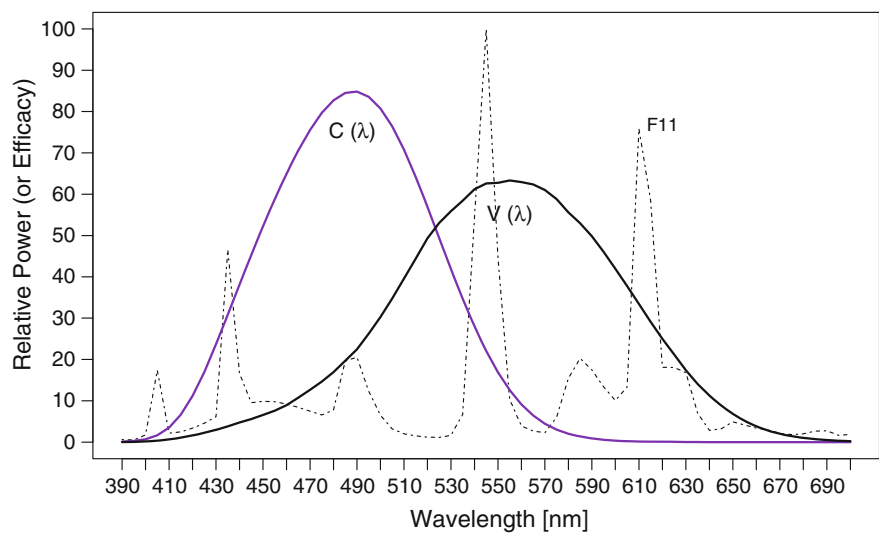


Fig. 2.13 Comparison of spectral response of the visual system (V -lambda) and the circadian system (C -lambda) to the spectral power distribution a narrow tri-band fluorescent lamp having a color temperature of 4000° K (the CIE illuminant F11)

Fig. 2.14 Mobile cart platform with laptop, HDR camera and CCD spectrometer



Fig. 2.15 Mobile cart showing spectrometer lens mounted adjacent to camera lens. The spectrometer lens is connected to the spectrometer via a 0.5 m fiber-optic cable



circadian system to light can be found in Amundadottir et al. (2013). These lighting related effects are of course overlaid on the myriad of physical and mental impacts in daily life that also effect alertness, performance etc. over time so that clearly disaggregating the lighting effects is a challenge. The framework developed by Andersen et al. (2012) includes a schema to segment the day into three discrete periods of analysis. These are, 6:00–10:00 AM (circadian resetting), 10:00–18:00 (alerting effects of daylight), and 18:00–6:00 (bright light avoidance, dim light only). Access to bright, circadian effective light in the morning is most critical for resetting the circadian system. Therefore, emerging CBDM metrics such as sDA or UDI are problematic for the assessment of circadian potential of a space because they do not account for the time during the day when a daylight stimulus is present. Analysis should prioritize the interval from 6:00 to 10:00 AM. However, it is important to note that exposure to bright light during the 10:00–18:00 period may be desirable (and preferred) by occupants for its potential to improve alertness. The task of developing novel daylight metrics and performance criteria specifically for the evaluation of circadian entrainment in buildings is discussed in Sect. 2.4.3.

2.4.1 Daylighting for Circadian Entrainment

Daylight is an attractive alternative to electrical lighting for maintaining human circadian entrainment indoors due to its spectrum (e.g. Fig. 2.12), intensity, general availability, and potential to be introduced into spaces via windows and skylights.

Enabling designs that ensure the appropriate spectrum, timing, intensity, and duration of light to maintain healthy circadian entrainment will require a new set of performance objectives, measurement techniques, and assessment tools.

The first step is to address how light is measured. Due to the difference in the spectral response of the circadian system (C-lambda) from the visual system (V-lambda), the standard unit of illuminance (photopic lux), is problematic for quantifying the lighting conditions required to reset the human circadian system (Lockley et al. 2003). A number of efforts have emerged to rationalize how lighting outcomes can be determined and assessed in biologically meaningful terms. Researchers have proposed models of the spectral sensitivity of the circadian system that can be used to relate the SPDs from various light sources to a stimulus effect (e.g. nocturnal melatonin suppression (Rea et al. 2012), or perceived alertness (Andersen et al. 2012)). The model developed by Rea et al., which is applied to assess the circadian stimulus potential of the spaces shown in Figs. 2.16 and 2.18, is based on published studies of nocturnal melatonin suppression using lights of various SPDs. The model relates a given SPD to a circadian stimulus effect from 0 (0%) to 0.7 (70%) characterizing the relative effectiveness of the source as a stimulus, assuming a 1-hour exposure time. A publically available circadian stimulus calculator is provided to convert various light sources to units of circadian light (CL_A) and Circadian Stimulus (CS) for relative comparison of light source spectra (LRT 2016).

Table 2.1 presents the predicted circadian stimulus effect from various light sources using the model developed by Rea et al. (2012). The table can be used to determine the level of vertical illuminance (lux) at the cornea that must be achieved to produce circadian stimulus effects ranging from 10 to 70% for daylight (D65, clear sky with sun) and three common electrical light sources: LED 2700 K, 34-Watt T-12 linear fluorescent, and Halogen 3277 K. For example, to achieve a 20% circadian stimulus effect, an occupant must be exposed to 103 lx of daylight (D65) at the eye over a period of one hour. To achieve the equivalent stimulus effect with light from a 34-Watt T-12 “cool white” linear fluorescent lamp, the eye-level vertical illuminance must be increased by a factor of three, to 306 lx. A present, Figueiro et al. (2016) recommend exposure to a CS of 0.3 or greater at the eye for at least 1 h in the early part of the day (equivalent to 180 lx, D65).

Table 2.1 Circadian stimulus effect from various light sources

(CS) (%)	D55	D65	D75	LED 2700 K	34WT-12LF	Halo. 3277 K
10	66	46	40	86	131	59
20	146	103	89	190	306	131
30	255	180	156	337	530	231
40	423	301	261	568	870	390
50	730	523	455	1005	1470	690
60	1520	1110	970	2220	2950	1520
70	127,000	98,500	89,000	NA	NA	NA



Fig. 2.16 Workspace illuminated with fluorescent lighting

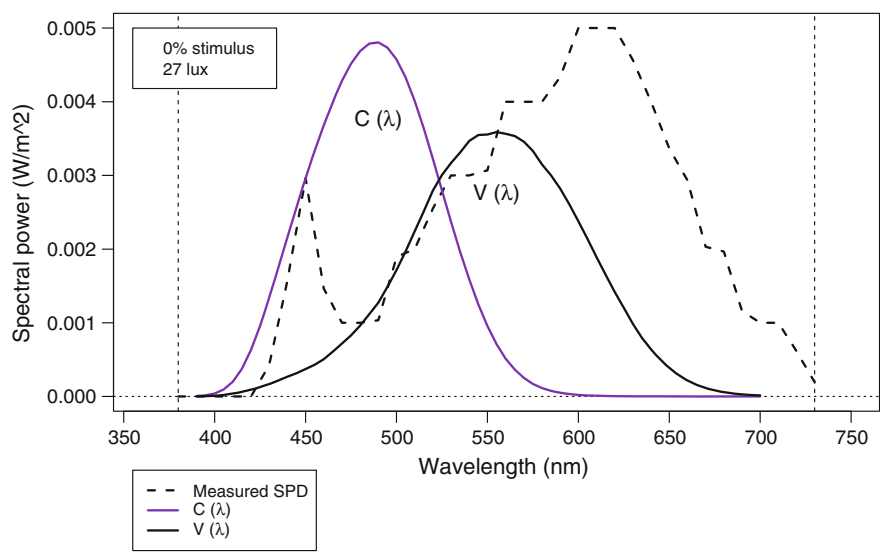


Fig. 2.17 Measured spectral power distribution, vertical illuminance (lux) and calculated circadian stimulus effect for Fig. 2.16 camera viewpoint

Alternatively, Lucas et al. (2014) have proposed a melanopic spectral efficiency function following the concept of melanopic illuminance introduced by al Enezi et al. (2011). Using a publically available calculator (Lucas et al. 2016), users can



Fig. 2.18 Workspace illuminated with daylight

calculate the resulting melanopic illuminance (lux) of various lighting conditions to understand and assess their biological impacts.

Researchers are also beginning to propose new approaches that seek to present a more holistic assessment of the effectiveness of a given lighting condition. For example, Rea and Bierman (2016) have proposed a universal luminous efficacy function (U-Lambda), which is proposed as a basis for setting light source efficacy requirements to serve multiple end user needs for light (e.g. color rendering, circadian regulation, scene brightness). Amundadottir et al. (2016) have proposed a unified framework to evaluate non-visual spectral effectiveness of light, which includes an online calculation and visualization tool (EPFL 2016) that can be used to compare the non-visual spectral effectiveness of various light spectra in terms of melatonin suppression, melatonin phase shift, and perceived alertness. Table 2.2 presents an example comparison of various common light source

Table 2.2 Biological impact of various light sources and photopic illuminances

Melatonin suppression (%)	EML	A (Lux)	F 11 (Lux)	D 65 (Lux)	LED 95 (Lux)
0.5	17	29	27	16	14
5	34	56	52	31	27
25	56	95	87	52	45
50	77	129	118	71	62
75	105	176	161	97	84
95	176	296	272	162	142
99.5	341	575	526	315	275

spectra (CIE A, CIE F11, CIE D65, and LED 95) in terms of Equivalent Melanopic Lux (EML), lux, and melatonin suppression (ranging from 0–99.5%). It should be noted that the framework developed by Amundadottir et al. incorporates a lens transmittance model to account for the relative loss in retinal exposure due to age of the observer. The outcomes presented in Table 2.2 are calculated assuming a 65-year-old observer.

2.4.2 *Field-Based Measurement Practices*

Because occupants are not well-equipped to report the circadian effectiveness of lighting conditions based on their own visual perception, and conventional photometric sensors are biased towards longer-wavelength light sources, new procedures are needed to measure and assess varying levels of circadian effectiveness, both during design and post-occupancy, where physical conditions may differ from design intent (e.g. due to window occlusion to control glare or increase visual privacy). And, the measurement condition must represent the conditions experienced by the human eye. This adjustment to conventional measurement practice creates several challenges, some of them obvious. First, the human eye is positioned vertically, requiring the measurement point to be oriented on a vertical, rather than horizontal plane. Second, occupants' viewpoints are likely to change over time, both regarding viewpoint location and view direction. Consequently, appropriate assumptions for the position and view direction of occupants are needed. Small changes to interior obstructions (e.g. partitions or furniture) can have large effects on levels of light reaching the eye. Consequently, it is a challenge to identify from what viewpoints in a space circadian effective lighting should be assessed, and what assumptions are most appropriate to account for potential obstructions. The challenge of view position is addressed in the examples presented in the following sections in context with additional parameters of light intensity, spectrum, duration and timing.

In the field, instrumentation capable of accurately measuring the SPD of light reaching the eye is needed to assess the relative effect of various light sources (and combined SPDs of multiple light sources) at various viewpoint locations in buildings. Figures 2.14 and 2.15 present one approach to address this need developed by the author, which uses a mobile cart platform to enable systematic evaluation of SPD in the field at adjustable eye-height levels (Burkhart and Konis 2016). The cart includes a digital Charge Coupled Device (CCD) spectrometer (model = OceanOptics JAZ-COMBO, effective range 300–750 nm, lens = cosine-corrected PTFE diffusing material) which is calibrated for measurements of absolute irradiance. The lens of the spectrometer is mounted adjacent to a High Dynamic Range (HDR) enabled CCD camera and connected to the spectrometer with a 0.5 m fiber-optic cable. The HDR camera enables point-in-time SPDs to be referenced to concurrent images acquired at near-identical viewpoints. These HDR images serve as a visual record of the scene and can be analyzed to evaluate glare and luminance conditions associated with SPD measurements.

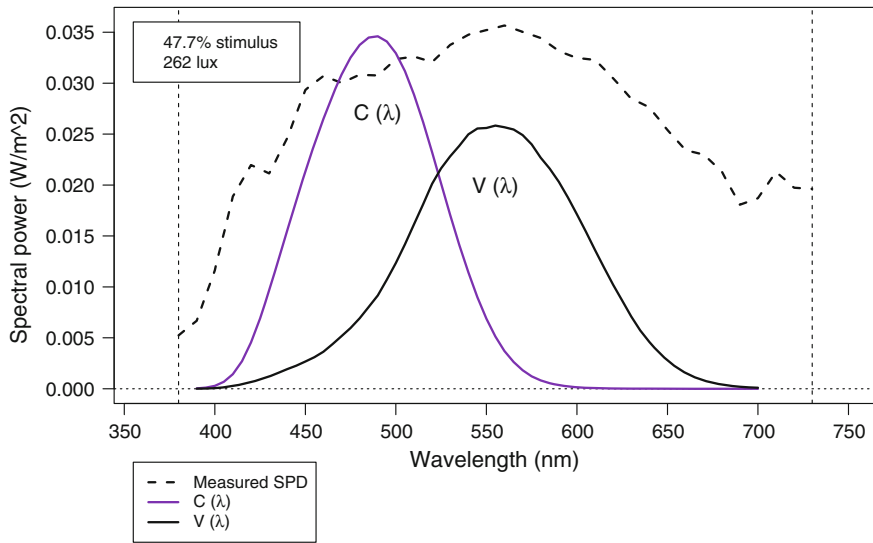


Fig. 2.19 Measured spectral power distribution, vertical illuminance (lux) and calculated circadian stimulus effect for Fig. 2.18 camera viewpoint

Figures 2.16 and 2.17 provide the outcome of a point-in-time evaluation using the mobile cart. Figure 2.16 shows a view of a work area illuminated exclusively by standard fluorescent lighting. The grey represents the luminous efficacy function ($V(\lambda)$) and the solid black curve indicates the response function of the circadian system ($C(\lambda)$). The measured global vertical illuminance at seated eye-level (27 lx) indicates that the light level is sufficient for photopic vision. However, note that the majority of the measured SPD falls outside the circadian response function ($C(\lambda)$) (Fig. 2.17). By applying the mathematical model developed by Rea et al. (2012) for quantifying circadian stimulus potential for a given SPD, which is based on a range from 0 to 70%, the lighting condition is found to be insufficient for circadian stimulus (0%). In contrast, Fig. 2.18 shows a similar work area illuminated exclusively with daylight. Despite the deployment of window shading devices on all windows, the measured global vertical illuminance at seated eye-level (439 lx) is higher, and the lighting condition is found to be sufficient to achieve a high level of circadian stimulus (55%) (Fig. 2.19).

2.4.3 Developing Circadian Daylight Metrics and Performance Criteria

There are currently no regulations governing lighting design to support circadian entrainment in buildings. Nor is there a consensus for the appropriate minimum light exposure threshold to ensure effective circadian stimulus, or for how long it must be

present. Designers interested in addressing the need for daylight access for circadian entrainment are faced with a translational challenge. Knowledge of the biological effects of light is based on a limited body of data and work from disciplines of neuroscience and photobiology, where translation of research outcomes to design practices is not direct or often clear. However, there is a growing interest in the development of guidance and requirements for circadian lighting. One such example is The Well Building Institute's WELL Building Standard (IWBI 2016). In order to evaluate and refine the performance of a given design, available scientific findings must be examined to establish criteria for the appropriate timing, intensity, duration, and spectrum of light required for effective circadian entrainment. Additionally, assumptions must be made for the patterns of occupancy and even the view directions of occupants in each space. The Well Building Standard includes a Circadian Lighting Design precondition (option 1) which implements a minimum threshold of 250 EML (equivalent to 226 lx from D65), assessed vertically at eye-level, which must be available for at least four hours each day and can be provided at any point during the day. While the current version of the WELL circadian lighting pre-condition is problematic in that it does not specify the time period during the day when an effective stimulus must be present, and overlooks the challenges and assumptions needed for assessments of light exposure at the eye, it represents an important first step in efforts to translate available scientific knowledge into performance requirements to better ensure that buildings effectively support the health and well-being of occupants. It anticipated that the specific requirements and criteria, and their underlying assumptions, will be revisited as the relationships between spectral distribution, duration, timing, and intensity of light exposure for optimal circadian health are further clarified by the research community.

Theoretical knowledge and scientific findings are now sufficient to explore how architectural designs can serve to orchestrate effective patterns of daylight for circadian entrainment. Questions remain for how to appropriately evaluate design outcomes. Recently, Inanici et al. (2015) developed a simulation procedure to more accurately compute the spectral content of light for the purpose of analysis using circadian lighting indicators such as EML or CS. The procedure is currently implemented in a software tool (Grasshopper plugin) entitled "Lark Spectral Lighting³" which can be used by designers to analyze luminance renderings and irradiance data to obtain point-in-time calculations of EML or CS. Yet, even with the capability to accurately simulate the spectral content of light for a given viewpoint, there is still the task of appropriately interpreting, summarizing and visualizing simulation outcomes to inform the design process. To address this need, a novel area-based circadian daylight metric for building design and evaluation has been developed by the author (Konis 2016), which can be used to assess and differentiate the performance of various daylighting strategies during the design phases of a project, or to examine existing spaces based on the frequency with which an effective circadian stimulus is present. An example application of the

³http://faculty.washington.edu/inanici/Lark/Lark_home_page.html.

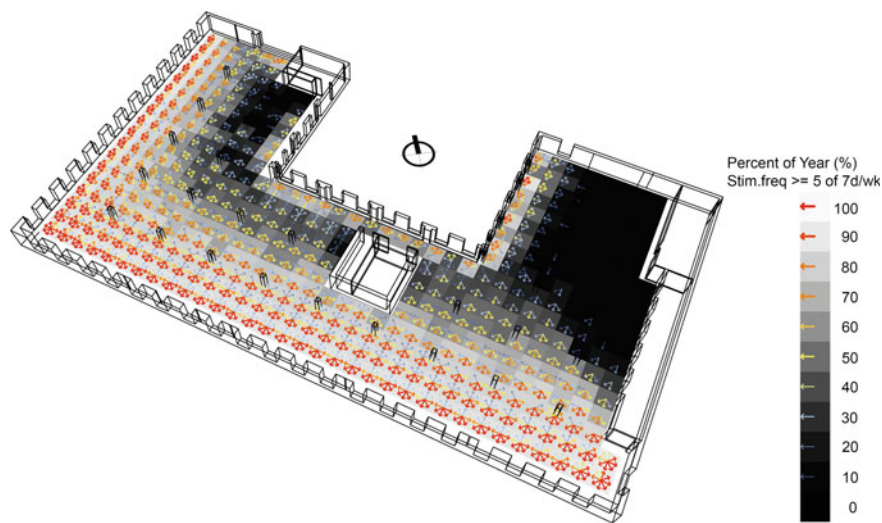


Fig. 2.20 Perspective view of building floor plate showing annual result for the percentage of analysis hours during the circadian resetting period (7:00–10:00 AM) where a minimum stimulus frequency of 71% (5 of 7 days/week) was achieved

metric is demonstrated in Fig. 2.20 through Fig. 2.23. Readers are encouraged to refer to the full paper (Konis 2016) for a detailed description of the metric and its calculation procedures.

Figure 2.20 shows the analysis result for a daylit office building floor plate located in downtown Los Angeles. A plan view is presented in Fig. 2.21. The geometry of the floor plate and fenestration is modeled after the location of the architectural design firm Perkins + Will's Los Angeles office. However, the example analysis presents the potential for daylighting prior to the addition of interior elements such as

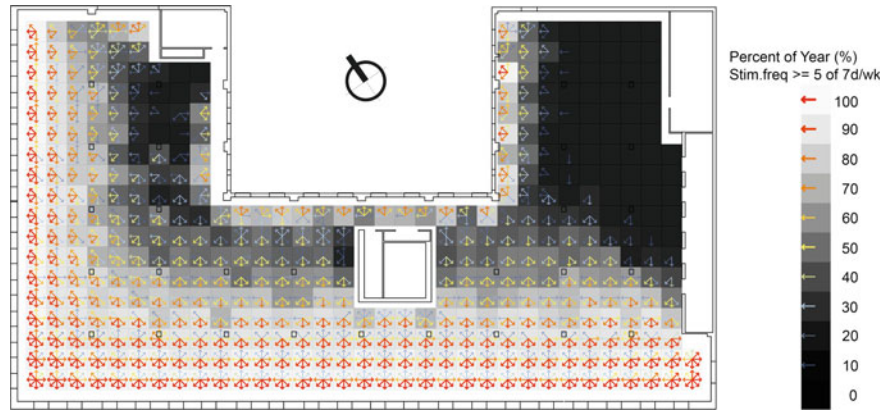


Fig. 2.21 Plan view showing same result as previous figure

non-structural walls, workstation partitions, or interior furnishings. Procedures using annual, climate-based daylight modeling of eye-level light exposures are applied to map the space in regard to the availability of a circadian-effective daylight stimulus.

Because the biological effects of light exposure are not instantaneous, a novel indicator (referred to as “stimulus frequency”) is applied to assess the frequency an effective stimulus is present over a window of time (e.g. 7-day period). While the minimum frequency needed to maintain healthy circadian stimulus is not known, it can be argued that measurement locations that have more frequent availability of an effective stimulus should be valued over those where availability is less frequent. The results in Fig. 2.20, reported for each view vector analyzed, show the percentage of the year where a stimulus frequency of at least 71% (5 of 7 days/week) is achieved. The daylighting potential of each location is then mapped based on the outcome of the best-performing vector (see Fig. 2.22). A stimulus is considered sufficient for a given day if a vertical light exposure of at least 250 EML is achieved throughout the portion of the circadian resetting period (7:00–10:00 AM) when the space is assumed to be occupied. Results can be used to identify and visually examine building zones where long-term occupancy may lead to disruption of the circadian system in the absence of supplemental electrical lighting capable of effective circadian stimulus.

Figure 2.23 presents an annual visualization of daylighting performance relative to varying levels (or grades) assigned to evaluate variations in levels of *entrainment quality*, where the “quality” of circadian entrainment is considered to diminish as the daily availability of an effective stimulus becomes less frequent over the moving 7-day analysis window. In Fig. 2.23, the percentage of analysis area falling into each *entrainment quality* grade category is reported on a scale ranging from 0 to 100% of the total analysis area. Designers can interpret Fig. 2.23 to understand seasonal changes in the spatial availability of a circadian stimulus as well as the

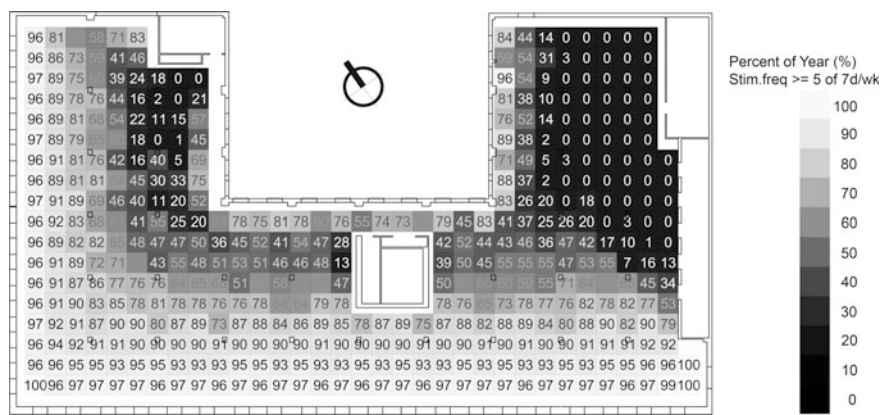


Fig. 2.22 Numerical mapping of the percentage of analysis hours during the circadian resetting period (7:00–10:00 AM) where a minimum stimulus frequency of 71% (5 of 7 days/week) was achieved

Fig. 2.23 Annual result showing daily variation in Circadian Effective Area (CEA) for each *entrainment quality grade* (A, B, C, D or F)

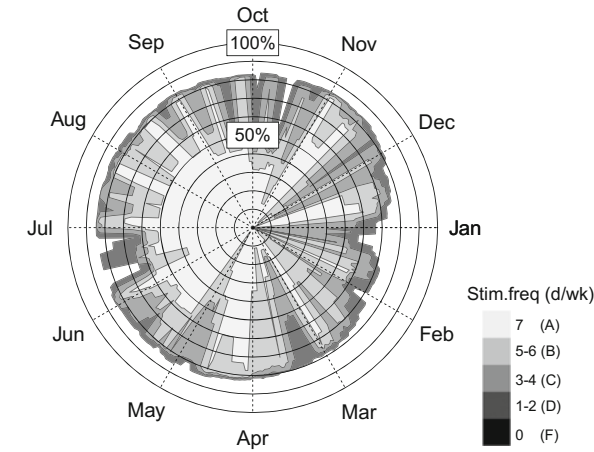


Table 2.3 Annual mean circadian effective area (0–100%) achieved for each *entrainment quality grade*

A	B	C	D	F
7d/wk	5-6d/wk	3-4d/wk	1-2d/wk	0d/wk
37.8	23.2	13.6	5.4	20

varying levels of *entrainment quality* achieved. For example, between the months of May to October, 40–50% of the analysis area achieves an *entrainment quality* grade of “A,” indicating that a stimulus is present on a daily basis (i.e. 7 days within any 7-day period) within this area. Similarly, nearly 80% of the analysis area is shown to achieve some level of effective stimulus for most of the year, however the entrainment quality is often lower (e.g. only available on 2 of 7 days at some locations) and more variable. The annual Circadian Effective Area (CEA) falling into each *entrainment quality* grade category is summarized in Table 2.3 and can be used to make relative comparisons between various daylighting strategies during design. For example, the design objective would be to increase the percentage of analysis area falling into the higher-grade categories (e.g. A and B) and minimize area within the lower categories (e.g. C, D and F).

2.4.4 Limitations and Future Directions of Circadian Daylighting

Understanding how buildings orchestrate 24-hour patterns of light and dark is a critical frontier of research for assessing and rating the Indoor Environmental Quality (IEQ) of a number of common building types. Theoretical knowledge, expert judgment and emergent scientific findings are sufficient to begin to propose performance criteria that have the potential to be achieved through thoughtful architectural design. This section described parallel ongoing simulation and

field-based efforts to examine the applicability of daylight the primary light source for circadian stimulus in buildings. The preliminary circadian daylighting metric (Konis, 2016) provides an important new capability to designers for quantifying and understanding the circadian potential of a given design as well as to identify biologically dark spaces in existing buildings, which require remediation or repurposing. The metric provides an additional objective for parametric simulation and optimization frameworks to rapidly explore and optimize the impact of a large combination of building parameters on the circadian potential of architectural space.

Unlike prior lighting and daylighting performance indicators, where applicability can be readily evaluated in the field by pairing physical measurements with occupant subjective assessments, the applicability of circadian daylight metrics for improving the health and well-being of occupants is much more complex, and will require novel methods to examine both short and long term health outcomes from daylighting design strategies in use. While these challenges are substantial, establishing feedback loops linking building design and occupant health outcomes is critical for improving quality of life in urban environments.

2.5 Visual Comfort

The balance of daylight transmission with the avoidance of glare is a central performance objective for effective daylighting. However, glare is rarely studied during the design process. This is largely due to the complexity of detecting and evaluating the dynamic patterns of luminance in daylight spaces and mapping how these patterns may affect the comfort and behavior of occupants. As noted in Sect. 2.2, maximum horizontal illuminance thresholds (e.g. 1000 lx), are currently implemented as proxy indicators for glare in CBDM metrics (e.g. UDI, sDA/ ASE). However, in modern work environments, visual tasks are often screen-based. With the visual task oriented vertically, direct view of the solar disc or extreme luminance contrasts between windows and indoor surfaces can often become sources of glare and are unlikely to correlate well (if at all) with measures of horizontal illuminance. As designers increasingly seek to improve access to daylight and window views for occupants, the ability to evaluate and address glare will be a critical factor in achieving effectively daylit spaces. This section discusses the potential and the limitations of existing and emerging approaches for evaluating glare.

2.5.1 Glare

Glare can generally be divided into three categories: (1) disability glare, (2) discomfort glare, and (3) veiling glare. Disability glare is defined as the disabling of the visual system to some extent by light scattering in the eye (Vos 1984) usually from very bright sources. Discomfort glare is defined by the IEA SHC Task 21 as:

“a sensation of annoyance caused by high or non-uniform distributions of brightness in the field of view.” Alternatively, the Commission Internationale de l’Éclairage (CIE) defines discomfort glare as: “visual conditions in which there is excessive contrast or an inappropriate distribution of light sources that disturbs the observer or limits the ability to distinguish details and objects.” Dynamic changes in lighting conditions that require rapid visual adaptation (e.g. from dark to light, or from light to dark) can also cause visual discomfort. Finally, veiling glare is the reduction in contrast of an image due to the reflection of a bright light source on the image, such as the reflection of bright windows on a computer monitor. Unlike disability glare, there is no well-understood mechanism for the cause of discomfort glare, although fluctuation in pupil size (Fry and King 1975) as well as distraction (Lynes 1977) have been suggested. Observation of daylit buildings in use often reveals the deployment of shading devices to address aspects of all three glare categories (e.g. Figure 2.24), which can in turn lead to significant reductions in daylight transmission, electrical lighting energy reduction, and visual connection to the exterior.

Figures 2.24, 2.25 and 2.27 present real examples of three common daylighting conditions that result in visual discomfort for building occupants. Lighting conditions were evaluated using a High Dynamic Range (HDR) enabled digital camera and software post-processing to produce calibrated luminance maps (Fig. 2.28) using a technique documented in (Konis 2012). This evaluation technique, and several of the most common metrics for glare analysis are discussed in detail in the following sections. Figure 2.24 shows a perimeter zone workstation where glare is caused by direct view of the solar disc. Despite the deployment of interior fabric roller shades, which supplement the additional solar control provided by an exterior perforated metal screen (50% openness) and solar control film (VLT = 0.23) applied to the facade glazing, the shade fabric openness factor of 0.03 (3%) is insufficient to completely block direct view of the solar disc, leading to luminances in excess of $50,000 \text{ cd/m}^2$ in the occupant’s field of view.

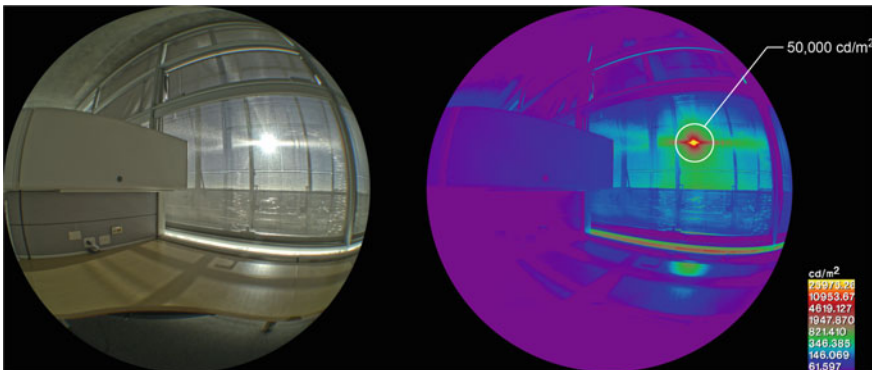


Fig. 2.24 Direct view of solar disc from perimeter zone workstation (*left*) and falsecolor luminance map (*right*)

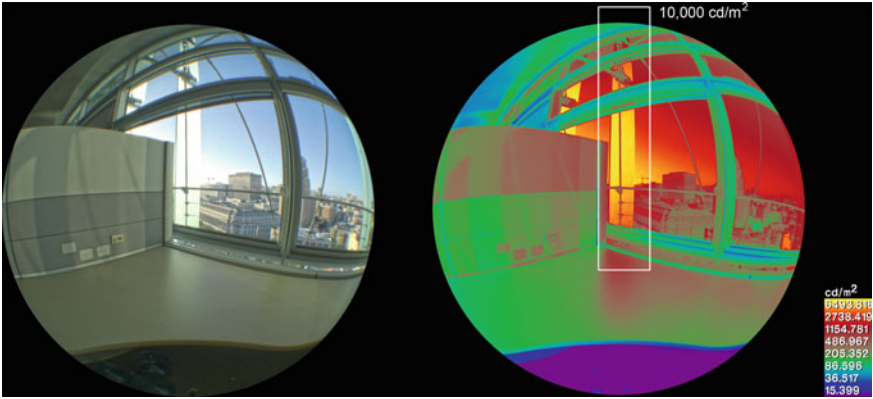


Fig. 2.25 View of exterior shading device surface in excess of $10,000 \text{ cd/m}^2$ from perimeter zone workspace

Fig. 2.26 Exterior view of translucent vertical louvers shown in Fig. 2.25



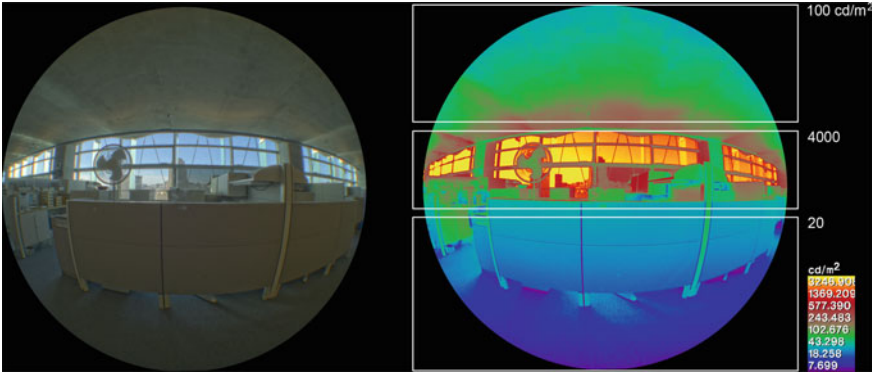


Fig. 2.27 View of facade glazing from core-zone of open-plan workspace in large daylit office building (*left*) and falsecolor luminance map highlighting contrast in luminance between facade glazing and interior surfaces

Fig. 2.28 Field installation of High Dynamic Range (HDR) enabled camera for acquisition of time-series measurements



Figure 2.25 shows an example where discomfort glare is produced from direct sun that is intercepted and diffused through the translucent louvers of an exterior shading system (Fig. 2.26). The louvers, when in direct sun, both reflect sunlight onto perimeter zone workstations (causing distracting luminance contrasts) as well as transmit diffuse light causing the entire louver surface to exceed luminance levels of $10,000 \text{ cd/m}^2$ on a daily basis. In comparison to Fig. 2.24, where visual discomfort was caused simply by the absolute magnitude of the glare source luminance, visual discomfort in Fig. 2.25 is caused by the excessive luminance contrast between the exterior fin surface ($10,000 \text{ cd/m}^2$) and the interior surfaces in the field of view ($\sim 200 \text{ cd/m}^2$), which result in a ratio of over 50:1.

The example presented in Fig. 2.27 shows the view of facade glazing from a viewpoint in the core-zone of open-plan workspace in large daylit office building. In this example, the contrast in luminance between facade glazing (4000 cd/m^2) and interior surfaces ($20\text{--}100 \text{ cd/m}^2$) exceeds a ratio of 40:1 and is likely to be a source of visual discomfort.

2.5.2 Daylight Glare Metrics

Concurrent with the reemerging interest in the daylighting of buildings in the 1960s, a study was conducted by (Hopkinson and Bradley 1960), to develop a metric to evaluate glare from large area sources (e.g. windows). The experimental setup consisted of a large illuminated diffusing screen (the light from the closely packed fluorescent lamps was diffused by an opal plastic screen), which provided a uniform luminance condition. The source size was varied from a small point source ($10\text{--}3 \text{ sr}$) to the whole field of view, and the source luminance was varied between 3.5 and $15,500 \text{ cd/m}^2$. Subjects reported their subjective impressions of glare on a scale ranging from “just perceptible” to “just intolerable.” The perception of glare depended not only on the brightness of the source but also on the size of the source as seen by the viewer, the viewers position relative to the source, and the surrounding scene luminance. The Daylight Glare Index (DGI) was derived and correlated to these subjective impressions.

$$DGI = 10 \log 0.478 \sum_{i=1}^n \frac{L_s^{1.6} \cdot \Omega^{0.8}}{L_b + 0.07 \cdot \omega^{0.5} \cdot L_s}$$

L_s source Luminance (cd/m^2)

L_b background Luminance (cd/m^2)

Ω solid angular subtense of source modified for the effect of the observer in relation to the source (sr)

ω solid angular subtense of source at the eye of the observer (sr).

Equation 1. The Daylight Glare Index (DGI).

The DGI can be applied to predict the level of visual discomfort from windows by providing values for the parameters identified above (Equation 1). The DGI was recommended by the International Energy Agency (IEA) Solar Heating and Cooling (SHC) Program Task 21 daylighting performance monitoring procedures (IEA 2000) as the appropriate metric for predicting visual discomfort in daylight spaces. However, a number of other glare metrics have been proposed for use in evaluating visual discomfort from windows. These include: (1) the Unified Glare Rating (UGR) (Einhorn 1998), recommended by the Commission Internationale de l'Eclairage (CIE) and the ASHRAE Performance Measurement Protocols (PMP) for commercial buildings (ASHRAE 2010), and (2) the CIE Glare Index (CGI) (Einhorn 1969, 1979).

Until the last 10 years all complex glare metrics involve variations of the same basic relationship between the four parameters of glare source luminance, solid angle subtended by the glare source, the angular displacement of the source from the observer's line of sight, and the general field of luminance (i.e. "background" luminance) (Equation 2).

$$Glare = \int \left(\frac{L_s^{a_1} \cdot \omega_s^{a_2}}{I_b^{a_3} \cdot P^{a_4}} \right)$$

L_s source Luminance (cd/m^2)

ω_s solid angle of source

L_b background Luminance/adaptation luminance

P Position index.

Equation 2. Relationship of the four parameters of glare used in complex glare metrics.

New research after 2000 resulted in the Daylight Glare Probability (DGP) (Weinhold and Christoffersen). The DGP (Equation 3) describes the fraction of disturbed persons, caused by glare from daylight and is reported over a range from 0 to 1, with three semantic thresholds: "imperceptible," "perceptible," and "disturbing" glare, corresponding to DGP values of (0.35, 0.40, and 0.45) respectively. The DGP equation was developed from statistical analysis on a dataset of human-factors assessments collected in daylight test facilities (full scale office mock-ups) at two locations (Copenhagen and Freiburg) with more than 70 subjects. In contrast to other complex glare formulae, the DGP equation adds a term for Vertical Eye illuminance (E_v), which was found to improve the correlation of the model with users' responses.

$$DGP = c_1 \cdot E_v + c_2 \cdot \log \left(1 + \sum_i \frac{L_{s,i}^2 \cdot \omega_{s,i}}{E_v^{a_1} \cdot P_i^2} \right) + c_3$$

E_v vertical Eye illuminance (lux)

L_s source Luminance (cd/m^2)

ω_s solid angle of source

P Position index

$$c_1 = 5.87 \cdot 10^{-5}$$

$$c_2 = 9.18 \cdot 10^{-2}$$

$$c_3 = 0.16$$

$$a_1 = 1.87$$

Equation 3. The Daylight Glare Probability (DGP) equation.

Recent research (Suk et al. 2013, 2016) has also explored simplified calculation methods aimed at providing clearer guidance for designers by identifying the basic elements of potential glare in a scene (absolute luminance and contrast ratio). Suk et al. define these as Relative Glare Factor (RGF) and the Absolute Glare Factor (AGF). Values obtained for each factor can be considered by designers to understand the dominant glare factor as well as predict the level of perceived discomfort through comparison to threshold values proposed by the researchers based on human-factors studies. Researchers have also begun to explore the application of multiple glare metrics in a multiple regression model and found that models combining multiple metrics predicted subjective visual discomfort better than a single metric alone (Van Den Wymelenberg 2012; Jakubiec et al. 2016).

2.5.3 Application of Glare Metrics Using HDR Images

In contrast to the relatively small, uniform, and stationary glare sources with constant brightness produced by electric lighting, the glare sources produced by windows vary in brightness, are constantly changing in size and position, and are usually distributed non-uniformly across a large area (e.g. a window or facade). Visual comfort calculations depend not only on the locations and brightness of light sources, but also on the apparent size of the light sources as seen from a particular viewpoint (Ward 1992). This presents a difficult measurement problem to researchers using conventional photometric instruments (e.g. masked illuminance sensors, or spot luminance meters) because the observer's entire field of view must be sampled in order to capture the luminance, position, and size of the glare source

(s) produced by the sky conditions. In addition, due to the non-uniform lighting distributions common in daylight spaces, the boundary of the glare source is more difficult to define. High Dynamic Range (HDR) images, by acquiring scene luminance data on a “per-pixel” scale, provide the ability to record the size, position and luminance of an arbitrary number of potential glare sources in the field of view, potentially enabling greater accuracy in the detection of dynamic glare sources.

Figure 2.29 presents the same glare examples presented in Figs. 2.24, 2.25, and 2.27 evaluated with the analysis program *evalglare*. Evalglare is a software program based on the studies of Weinold and Christoffersen (2006) and was developed to detect and evaluate glare sources within a 180° hemispherical image given in the Radiance image format (.pic or .hdr). Evalglare reports the DGP for the given scene in addition to a number of other common glare metrics and includes a number of input parameters that can be manipulated to adjust the predicted outcome. The most significant input assumption is the specified threshold factor for glare source detection that can be a constant value (e.g. all regions that exceed 1000 cd/m²), or a multiple of the average visual task luminance (e.g. all regions that exceed seven times the average luminance of a user-specified visual task area), or a multiplier of the average luminance of the entire scene (if no task view is given). The program operates with a default assumption that all regions that exceed 5 times the visual task (or entire scene) should be treated as a glare source. Figure 2.29 compares the original .hdr image (left) with the check file produced by Evalglare (right), using the “cut” field of view according to Guth, which presents the total field of human vision as limited by facial structure.

2.5.4 Dynamic Glare Evaluation

While a single “point-in-time” evaluation of glare may be valuable for static lighting environments, it offers limited feedback on the success or failure of a given daylighting design over daily and seasonal changes in sun and sky conditions. Understanding visual comfort performance requires assessing the time-varying patterns of luminance from specific views, including the effect of active shading use, and making assumptions for how daily and annual patterns impact occupant acceptance and behavior. As a simple example, Fig. 2.30 presents a daylight scene from a real building over the course of 12 h in one day under predominantly clear sky conditions. Figures 2.31 and 2.32 show the calculated DGI and DGP outcomes at 5-minute intervals derived from HDR images acquired on site. Notably, the DGI and DGP daily profiles vary in their prediction of the severity of glare, with the DGP predicting glare exceeding the “disturbing” semantic threshold in the morning and afternoon (Fig. 2.31) and the DGI predicting a level of glare above “just acceptable,” but below “just uncomfortable” (Fig. 2.32). While the glare metric predictions vary considerably throughout the day, it is unlikely that occupant comfort and acceptance change at the same rate, or correlate directly with “point-in-time” predictions. It is far more likely that occupants will form opinions about the visual comfort of their environment over a much longer time period, and

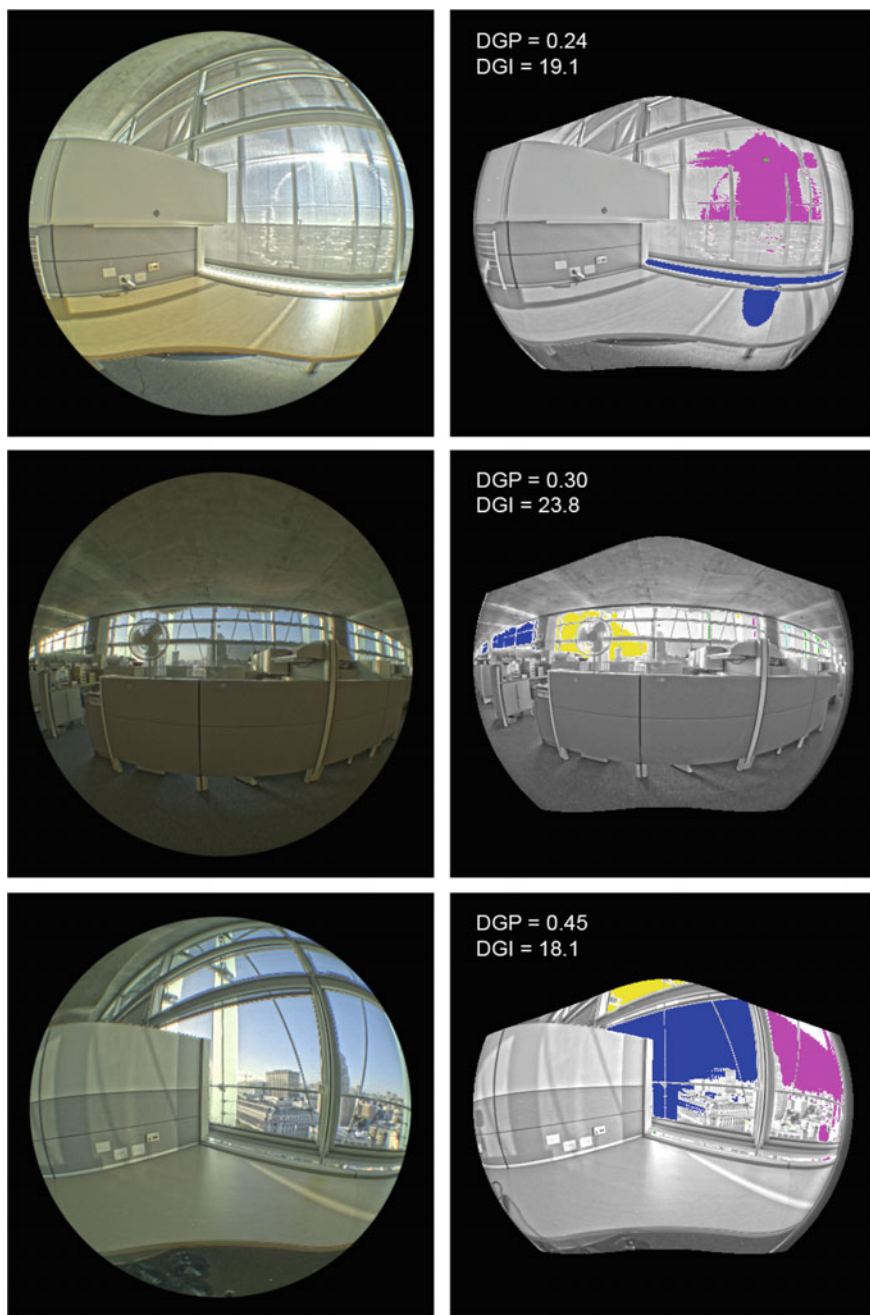


Fig. 2.29 Example field of view modification, glare source detection, and glare prediction (DGP and DGI) performed by the *evalglare* software tool on HDR images of real daylit scenes. Arbitrary colors are used to identify the glare sources detected

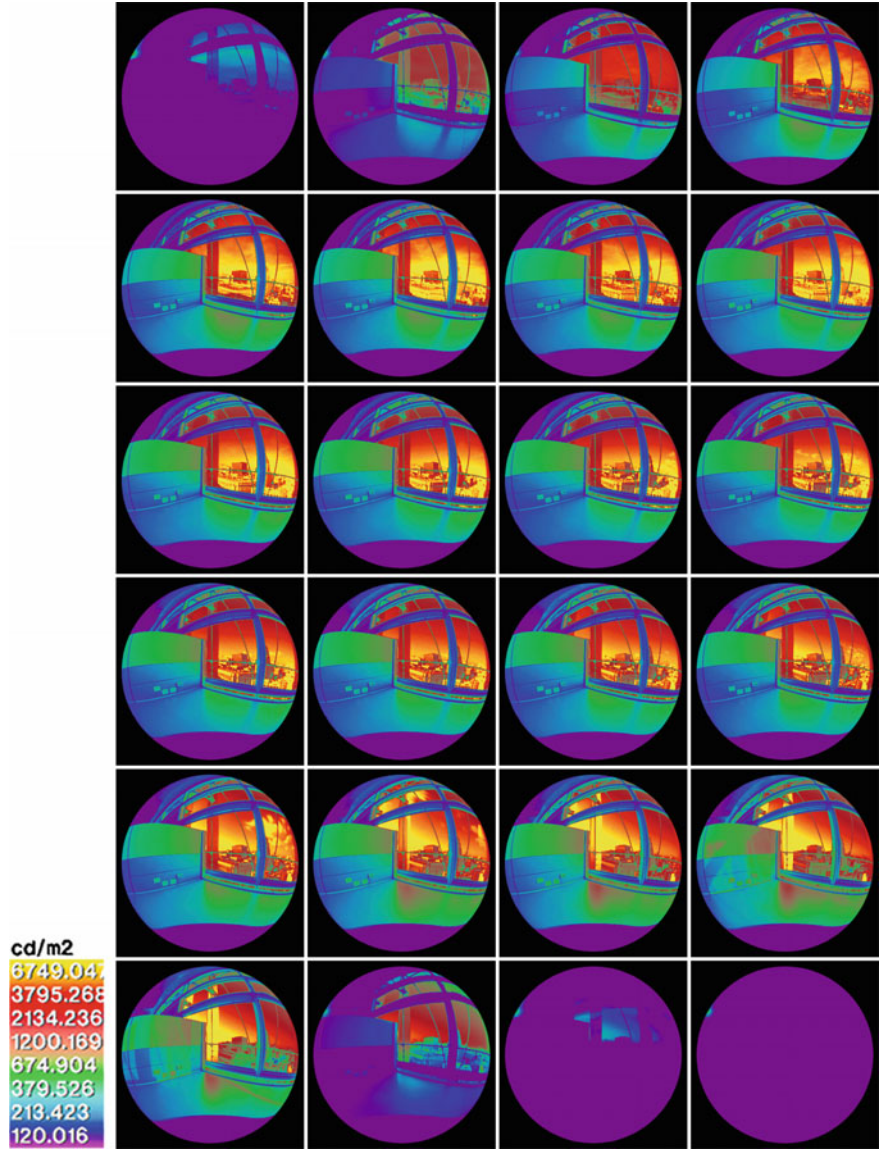


Fig. 2.30 Time-series representation of daily luminance pattern for window facing view from Fig. 2.25. An image is shown at every 0.5 h from 6:30 AM to 6:00 PM Standard Time October 25, clear sky conditions

will both adapt to, and modify their environment to reduce visual discomfort. The most common adaptation is to turn ones head away from the worst glare source and to lower available shading devices, which, if manually operated, are rarely retracted when the source of glare is no longer present.

Fig. 2.31 Time-series DGP prediction based on *evalglare* analysis of 5-minute interval HDR image data

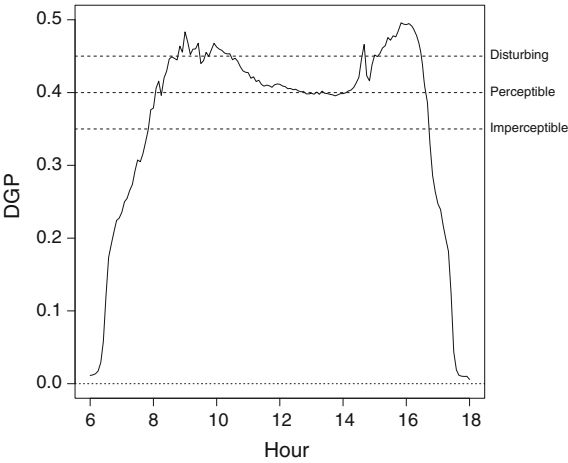
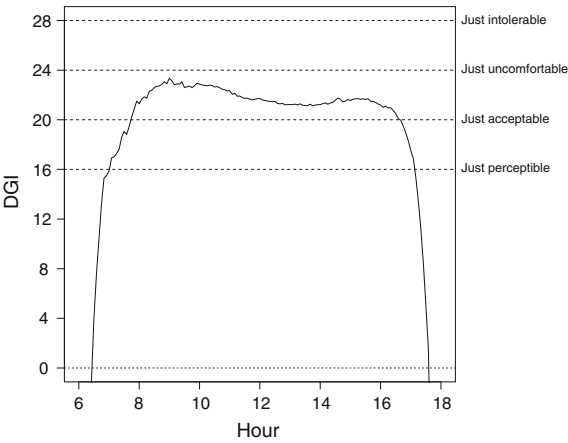


Fig. 2.32 Time-series DGI prediction based on *evalglare* analysis of 5-minute interval HDR image data



2.5.5 Frequency and Magnitude of Glare

In an effort to examine the frequency and magnitude of glare over various time periods (e.g. week, month, year), Weinold developed Dynamic Daylight Glare Evaluation (DDGE) (Weinold 2009). The approach applies the evalglare tool to time-series sets of images from a given viewpoint within a space. Time-series results for a specified period (e.g. annual, occupied hours) are then ordered by magnitude and examined relative to various proposed daylight glare “comfort classes.” Class A, B, and C are used as a basis to differentiate performance outcomes as shown in Table 2.4. To visually examine the daily and seasonal occurrence of varying levels of glare for a particular viewpoint, Jakubiec integrated

Table 2.4 Daylight glare comfort classes defined by Weinold (2009)

	A	B	C
	Best class	Good class	Reasonable class
	95% of office-time glare weaker than “imperceptible”	95% of office-time glare weaker than “perceptible”	95% of office-time glare weaker than “disturbing”
DGP limit	≤ 0.35	≤ 0.40	≤ 0.45
Average DGP limit within 5% band	0.38	0.42	0.53

Both limits (DGP, and average DGP within 5% band) must be fulfilled



Fig. 2.33 Annual Daylight Glare Probability (DGP) simulation. The x-axis corresponds to 365 days of the year, the y-axis corresponds to time of day. *Red* and *orange* fields correspond to hours with intolerable or disturbing glare, respectively, *yellow* to perceptible glare and *green* to imperceptible. *Image credit* Alstan Jakubiec



Fig. 2.34 Annual Daylight Glare Probability (DGP) simulation result for window-facing view orientation. *Image credit* Alstan Jakubiec

DDGE into the software DIVA-for-Rhino (Jakubiec and Reinhart 2012), to generate annual glare maps. Figure 2.33 presents an example of an annual outcome for a task-facing view. For comparison, Fig. 2.34 presents the annual result for the same location, but with a window-facing view.

2.5.6 View-Direction Dependent Glare Evaluation

To predict glare discomfort in open-plan office environments, it is necessary to evaluate all significant views in regularly occupied spaces within a project. This requires that dynamic glare evaluation include multiple view positions and, due to the ability of occupants to adjust their view direction, a range of view vectors from each position. To address this latter challenge, Jakubiec and Reinhart (2011) developed a concept called the “adaptive zone” and a simulation-based approach where cylindrical images (a 180° vertical, 360° horizontal view) overlaid with a view direction-dependent glare evaluation are used to predict levels of discomfort glare for a user-specified range of view orientations. Individual images can be composited into animations that can be used by designers to visualize the directionality of glare for a specific location (and range of view directions) of interest within a project. Figure 2.35 shows an individual “point in time” cylindrical representation of view and corresponding glare predictions for various available view directions. Jakubiec and Reinhart found that by applying the adaptive zone concept to a sidelit office with manually operated venetian blinds it was possible to “reduce the predicted hours of intolerable discomfort glare from 735 to 18 occupied hours per year and increases the annual mean daylight availability from 40 to 72%”. Figures 2.36, 2.37 and 2.38 show view-direction dependent glare evaluations for Gund Hall, (Harvard Graduate School of Architecture), at various times during the year. The bars across the bottom of each image illustrate predicted levels of discomfort glare in the indicated orientation for each analyzed metric (green = imperceptible, yellow = perceptible, orange = disturbing, red = intolerable).

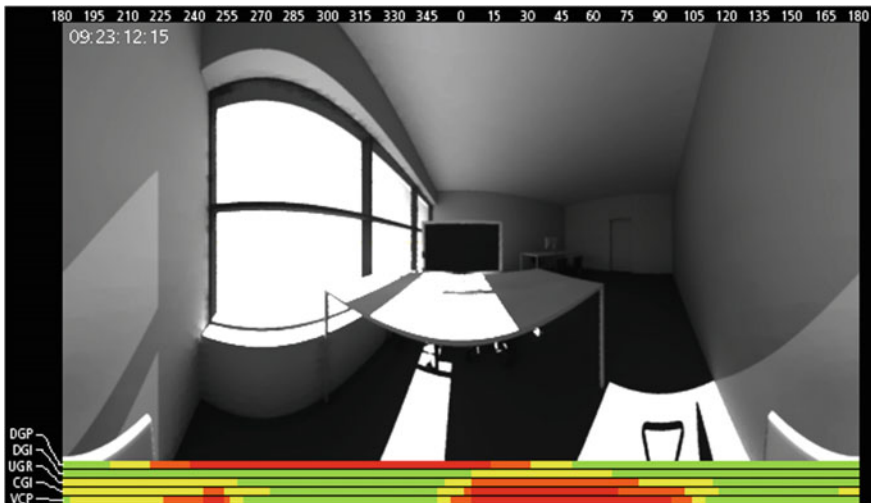


Fig. 2.35 View-direction dependent glare evaluations on September 23 at 12:15 PM in sidelit office space. *Image credit* Alstan Jakubiec

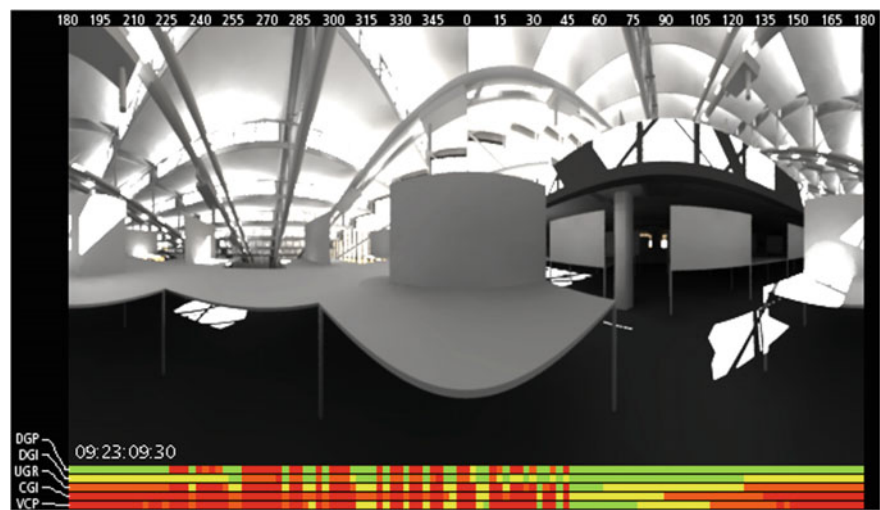


Fig. 2.36 View-direction dependent glare evaluations on September 23 at 9:30 AM in a large open-plan work space. *Image credit* Alstan Jakubiec

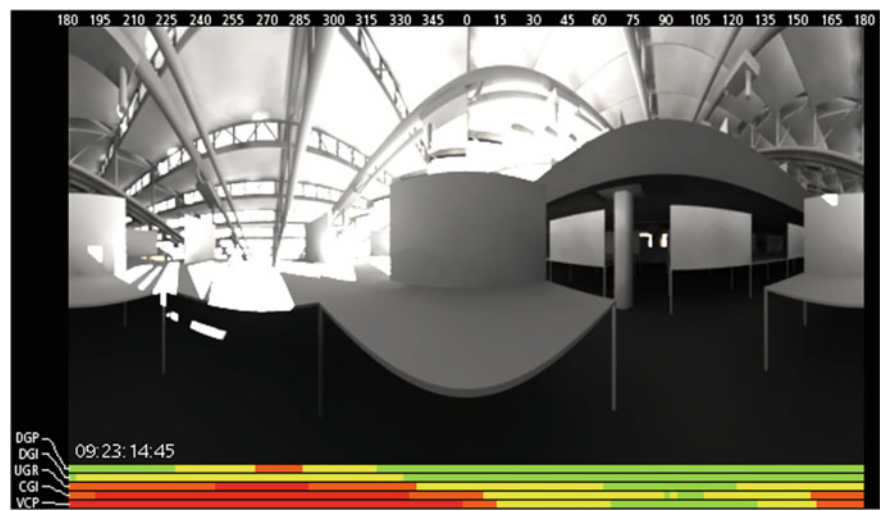


Fig. 2.37 View-direction dependent glare evaluations on September 23 at 14:45 AM in a large open-plan work space. *Image credit* Alstan Jakubiec

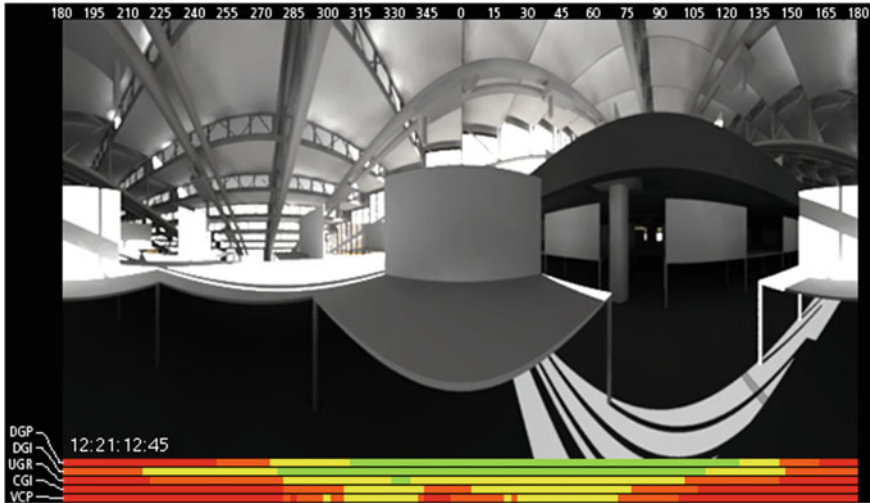


Fig. 2.38 View-direction dependent glare evaluations on December 21 at 12:45 AM in a large open-plan workspace. *Image credit* Alstan Jakubiec

2.5.7 *Limitations and Future Directions of Visual Comfort Evaluation*

The development of better methods and tools to predict visual discomfort in daylit spaces remains an active research topic. Currently there is no widely agreed-upon method to accurately predict discomfort glare in daylit environments. And while a single “point-in-time” evaluation of glare may be valuable for static lighting environments, it offers limited feedback on the success or failure of a given design over daily and seasonal changes in sun and sky conditions. Understanding visual comfort performance requires assessing the time-varying patterns of luminance from specific view positions and making assumptions for how hourly, daily and seasonal patterns impact occupant behavior and shade use. While quantitative, simulation-based methods have been developed, assumptions relating annual exposures to occupant outcomes are largely derived from very limited (and much shorter-term) laboratory-based occupant studies or on expert judgment rather than on extensive field validation. Further inquiry is needed to evaluate how occupants adjust shading and make other behavioral modifications in daylighted spaces, as well as how they form long-term opinions of visual comfort in dynamic daylit environments that include varying levels of glare, and how occupants prefer to manage trade-offs between levels of glare and other IEQ factors, such as access to a window view or higher daylight levels. For example, research by Tuaycharoen and Tragenza (2007) indicates that the absolute tolerance of glare from windows is related to the visual content of the view through the window, where higher predicted DGI values will be tolerated for views rated positively. This supports studies

from the 1960s when glare ratings based on electric lighting were first being adapted for use with daylight. One significant challenge in the application of computing annual climate-based daylighting metrics, modeling of occupant behavior and luminance-based glare analysis is in the development of equally complex Post Occupancy Evaluation (POE) mechanisms capable of validating the large collection of assumptions embedded in annualized performance outcomes.

Rather than working to establish a consensus for the most effective glare metric, behavioral model, or equation for annualizing the results of hourly daylighting simulations, designers may forgo a universal design paradigm based on a theoretical “standard observer” and begin to apply existing metrics and analysis tools to develop personalized, data-driven comfort models, drawing on the increasing availability of sensor feedback from real daylit spaces in use. For example, luminance maps acquired from low-cost HDR imaging devices (e.g. LBNL SkyCam), paired with contextual, behavioral and subjective data, can be analyzed on embedded computers to determine unique, real time comfort models. With enough data and time, these models might generate algorithms based on measured data that inform selection and optimization of the major design parameters. These models, in turn, can be shared within the design profession to improve understanding of user experience in buildings, as well as to inform the operation of dynamic glare control systems in the buildings themselves.

It is important to keep simulation outcomes in context with a holistic set of design options. For example, completely blocking the solar disc at the facade with 3-dimensional exterior screen may achieve the same visual comfort outcome as a simple, thoughtfully designed adjustable shade integrated into a workstation partition. The latter option provides occupants with personal task-level control over a thoughtfully considered dynamic range of lighting conditions, while maintaining views and transmission of sufficient ambient daylight to meet IEQ and energy objectives.

2.6 Visual Connection to the Outdoors

Greater emphasis on the provision of access to window views for all occupants is helping to invert conventional practices for the space planning of office buildings, placing open-plan offices along the perimeter of the floor plate and locating enclosed cellular office space in the core. For larger buildings, view requirements for the majority of regularly occupied space necessitate a transition from relatively “fat” floor plate buildings with a low surface-to-volume ratio to “thinner” more elongated building forms, with a higher ratio of surface-to-volume and often a more complex form. Finally, in addition to encouraging thinner floor plates, the adoption of emerging metrics aimed at quantifying and rating available views, such as the “view factors” now being adopted by voluntary rating systems like LEED, are a further incentive for designers to apply floor-to-ceiling facade glazing in order to

achieve compliance for deep floor plate buildings, creating significant technical challenges for managing thermal and visual comfort along the perimeter.

Interest in the provision of views for all occupants is driven by a large body of research in the field of environmental psychology that supports the conventional wisdom that the provision of windows is an essential component of occupant performance, health, and well-being. In an effort to characterize these benefits, Collins (1975) conducted a review of available literature and reported windows serve a number of psychological functions, including view, stimulation, and the perception of spaciousness in addition to the provision of sunlight and daylight which were both shown to be desired by building occupants. Collins additionally reported that the absence of windows in spaces that were confined or static could result in adverse reactions from occupants. Later research in windowless workspaces by Heerwagen and Orians (1986) showed that occupants frequently decorate a windowless office with posters of outdoor scenes as a means of creating a “surrogate” window. Figure 2.39 presents an example of a “surrogate window” (right) installed in a medical office building. A staff member installed the “surrogate window” on the back surface of a sign directly in front of her field of view (left). The “surrogate window” is a detailed photograph of a large redwood tree surrounded by a forest landscape. What is notable about this example is that the view position is approximately 12 m from the facade and includes a large window view of an adjacent building, which delivers significant levels of daylight. An informal interview of the staff member revealed that “surrogate window” was installed due to the perceived poor quality of view content provided by the window. This individual example supports the theory presented decades ago by MC Lam in his seminal work, *Perception and Lighting as Formgivers for Architecture* (Lam 1977), where



Fig. 2.39 Example of a “surrogate window” (right) installed in a medical office building. A staff member installed the “surrogate window” on the back surface of a sign directly in front of their field of view (left)

Table 2.5 Biological needs for environmental information, after Lam (1977)

Location	With regard to water, heat, food, sunlight, escape routes, destinations, etc
Time	And environmental conditions which relate to our innate biological needs
Weather	As it relates to the need for clothing and heating or cooling, the need for shelter, opportunities to bathe in the beneficial rays of the sun, etc
Enclosure	The safety of the structure, the location and nature of environmental controls, protection from cold, heat, rain, etc
The presence of other living things	Plants, animals, and people
Territory	Its boundaries and the means available within a given environment for the personalization of space
Opportunities for relaxation and stimulation	Of the mind, body, and senses
Places of refuge	Shelter in time of perceived danger

he outlines a list of important biological needs for environmental information (Table 2.5), which go far beyond the provision of view. If these needs are not well served by designers, occupants will make modifications to the extent possible to better serve these various needs.

In addition to the availability of a view, the content of the view is shown to have an effect on psychological well-being. The most consistent finding is the preference for natural over built views (Farley and Veitch 2001). Windows with natural views were found to enhance work and well-being in a number of ways including increasing job satisfaction, interest value of the job, perceptions of self-productivity, perceptions of physical working conditions, life satisfaction, and decreasing intention to quit and the recovery time of surgical patients (Farley and Veitch 2001). The view of a natural scene through a window (either real or simulated) has also been proposed as a means of relieving stress (Kaplan 1993; Ulrich 1991). The content of the view can also affect the preference of occupants towards the size and shape of the window, with relatively smaller windows being acceptable for distant views and larger windows required for views of nearby objects (N'eman and Hopkinson 1970). Studies have also shown that access to a window view can have a measurable relationship to changes in office worker performance. In a field-based investigation conducted in two large office buildings in California, the Heschong Mahone Group reported that better access to a window view was found to consistently predict better performance (CEC 2003).

Access to a distant view has also been linked to eye health. In modern office environments where workers spend increasing amounts of time viewing computer screens or workstation partitions, the distant view provided by windows allows changes in eye focus distance to give the eye muscles a chance to relax. Because the focus distance required for ocular muscles to relax is significantly greater than the dimensions of most buildings, a window view of distant scenery provides an important alternative focus for the eyes.

Given the body of research on the importance of window view for occupant health and well-being, the provision of a satisfactory level of visual connection to the outdoors through window views is a critical performance objective. A number of parameters can be considered evaluating view. These can be separated into factors considering the availability, amount, and quality of visual connection to the outdoors. Each parameter is discussed in the following sections.

2.6.1 Window Size and Aperture Configuration

Many European and Scandinavian building standards include provisions for view, which are often incorporated with daylighting requirements. One such example, first published in 1935, is the German Standard on daylighting (DIN 5034, “Daylight in Interiors”). Part 1 of DIN 5034 specifies minimum window sizes based on room size as well as requirements for the configuration of the window aperture. According to DIN 5034-1 (2011), the top edge of visually transparent window glazing must be a minimum of 2.2 m (7.21 ft) above the finished floor height, and the bottom edge cannot exceed 0.9 m (2.95 ft). In addition, the sum of window widths must meet or exceed 55% of the room width, leading to a minimum window-to-wall ratio requirement of approximately 30%.

While provision of a window view is not a requirement for office buildings in the U.S., the desire to specify view requirements in green building rating systems has led to a need to define measurable criteria for window views. In the current version of LEED (v4) (USGBC 2016), the concept of a “view factor” is introduced, based on a study of office worker performance and the indoor environment (CEC 2003). Calculations of the view factor result in a numerical score from 0 to 5 determined by the smaller of the lateral and vertical view angles for a specified viewpoint. As defined in the report: “A view rating of 5 almost completely filled the visual field of the observer seated at the cubicle. A view of 4 filled about one-half of the visual field. A view of 3 represented about one-half the size of a view 4, but still with a coherent view. A view rating of 2 represented a narrow and typically fractured view. A view rating of 1 represented a glimpse of sky or sliver of the outside environment.” Table 2.6 provides minimum view angles for each view factor score. Compliance with the view factor option in the current version of LEED (v4) requires a view factor of 3 or greater. Figure 2.40 shows the lateral and vertical view angles achieved for a viewpoint located 3 m (9.8 ft) from the facade, which results in a view factor of 4. While the original view factor scores were determined from observational studies including moveable furnishings and other obstructions common in office spaces after occupancy, the LEED calculation procedure allows for non-permanent obstructions to be excluded (Fig 2.41).

Table 2.6 View factors

View Factor	View angle	
	Min-max (°)	Gray zone range (°)
1	1–4	
1 or 2		4–5
2	5–9	
2 or 3		9–11
3	11–15	
3 or 4		15–20
4	20–40	
4 or 5		40–50
5	50–90	

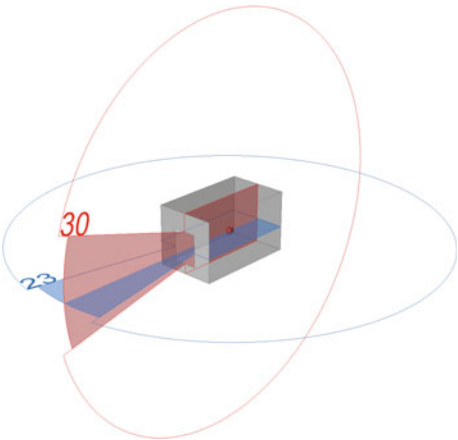


Fig. 2.40 Lateral and vertical view angles achieved for a viewpoint located 3 m (9.8 ft) from the facade

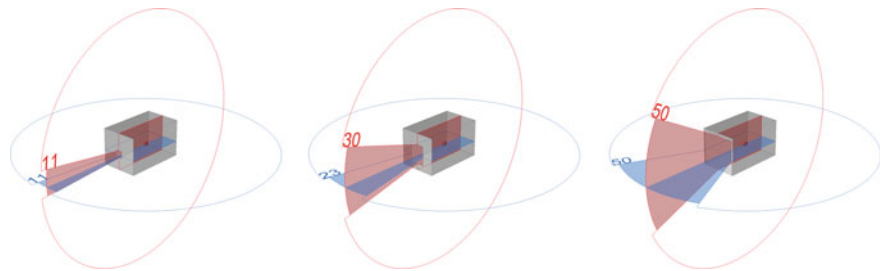


Fig. 2.41 View factors of 3,4,5 for a seated view-point 3 m from the facade

2.6.2 Distance of Occupants from Windows

The distance of occupants from windows is another important parameter for assessing visual connection to the outdoors, and has significant implications for building form. For example, DIN 5034 (2011) requires that all workspaces must be located within 10 m of a window. This limit restricts the floor plate depth of German office buildings, leading to relatively “thinner” forms than their U.S. counterparts, and more frequent use of courtyard and atria formal arrangements due to the greater ratio of skin to volume. While not an explicit distance limit, the LEED requirement to provide, “unobstructed views located within the distance of three times the head height of the vision glazing,” leads to a similar distance limit of approximately 10 m from windows for typical finished floor-to-ceiling heights (e.g. 3 m). The Nordea Bank Building (Fig. 2.42), designed by Henning Larsen Architects, presents a contrast to typical large commercial office building planning. A primary objective of the building form is to provide the best opportunities for all of Nordea’s employees to work in an environment connected with daily and seasonal changes in daylight and views to the outdoors. Atriums are placed in the center of the building mass and serve to spatially connect the first floor (level 01) to the upper floor (level 07) creating a feeling of unity between the various work zones within the large project. The open place offices are arranged along the exterior of the floor plates adjacent to the facade, providing a direct visual connection to the exterior environment for all regularly-occupied work areas (see Chap. 5 for a more detailed description of the project).

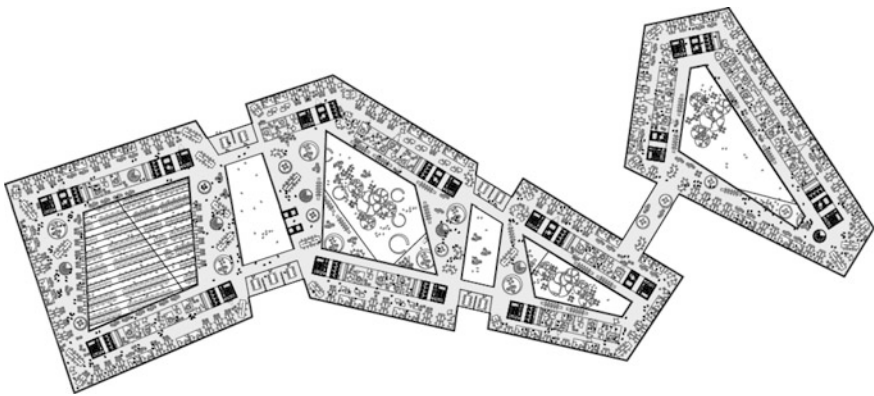


Fig. 2.42 Nordea Bank Headquarters typical *upper* level floor plan. *Image credit* Henning Larsen Architects

2.6.3 Provision of Multiple Views

The number, direction, and aggregate view angle of available window views can also be used to evaluate the view potential from a given location. Providing multiple views can enable greater awareness of exterior phenomena (e.g. changes in weather, activities) as well as provide more diverse visual content (e.g. both urban and natural views). Perhaps the most practical benefit of views from multiple directions is the possibility of preserving an unshaded window view when other views require shading for solar and glare control. The quantity of views can be evaluated using a number of indicators including (1) the total number of distinct window views, (2) the total visual angle of available window views, as well as the distribution of views over the occupant's horizontal field of view. For example, the LEED v4 compliance option requires, "multiple lines of sight to vision glazing in different directions at least 90° apart." The available number of views should be considered in context of the occupant's primary visual task view, if known. For example, the views available from the occupant's primary task view (while seated) may be valued higher than the views available when standing and/or looking away from the primary visual task. Figure 2.43 shows an example analysis for one test point located at seated eye-height on an open-office floor plate. The analysis uses a view rose technique to visualize the total number of window views, the horizontal view angle of each view, and the total horizontal view angle (119 of 360°) by

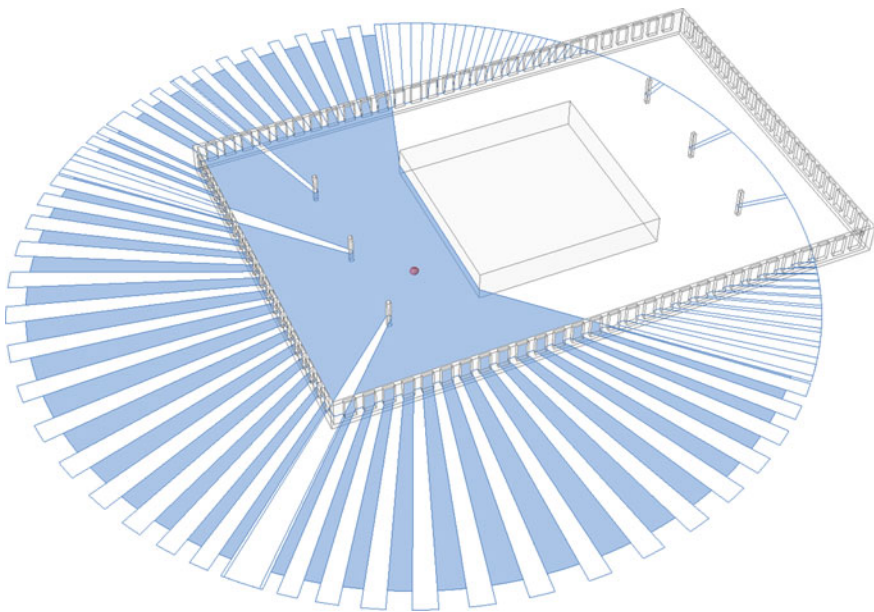


Fig. 2.43 Example line-of-sight analysis for a specified workstation location in an open-plan office floor plate. Analysis was performed using the “view rose” component in Ladybug

determining the direct lines of sight reaching a specified distance from the test point (e.g. 40 m).

2.6.4 View Content

Attributes of view content can also be used to evaluate view quality. For example, Fig. 2.44 compares a view of a traditional Chinese garden (The Garden of Flowing Fragrance, Liu Fang Yuan⁴ (left), with a view of blank wall opposite a narrow daylight void space (right). The view of the garden includes a number of key attributes that contribute to a quality view. These include view of (1) flora and fauna, (2) the sky, and (3) movement (e.g. surface of water, branches and leaves of trees), (4) the presence of people, and (5) a distant view. These attributes, in addition to many others, help to enable a complex emotional process defined by the eminent biologist Edward O. Wilson as *Biophilia*: “the innately emotional affiliation of human beings to other living organisms” (Wilson 1986, p. 31). Recognizing that attributes such as these are undervalued in conventional design practices relative to their importance for maintaining human psychological well-being, scholars have worked to develop and identify *biophilic design* practices (e.g. Kellert and Heerwagen 2008) as well as include requirements for view content into green building compliance criteria. For example, the current version of LEED requires that, “views that include at least two of the following: (1) flora, fauna, or sky; (2) movement; and (3) objects at least 25 feet from the exterior of the glazing.” While designers can rarely construct natural landscape settings, designers can survey the visual assets available for each project using the attributes of biophilic design as a filter to prioritize the organization and orientation of program space and building form.



Fig. 2.44 Window view to a high-quality view content (traditional Chinese garden), (left). Window-view to low-quality view content (adjacent blank wall), (right)

⁴<http://www.huntington.org/chinesegarden/>.

2.6.5 Visual Transparency and Openness Factor

For fenestration systems with interior or exterior solar and glare control elements that screen or partially occlude the window view, the openness factor is an additional parameter with significant impacts on view quality. Control of excessive solar heat gains is one of the primary challenges for low energy daylit office buildings. While designers can easily reduce window size and add coatings or solar control films to reduce solar gains, contemporary designers rarely take this approach due to the negative impacts on daylight availability and views. Instead, designers are increasingly using exterior solar control screens over large areas of facade glazing to reduce solar loads while creating larger window views that preserve screened or partially-occluded views for occupants. Figure 2.45 shows an example of the perforated metal screen used for solar control on the southeast-facing facade of the San Francisco Federal Building. The screen is composed of small, regularly-spaced circular perforations which achieve a 50% openness factor at normal incidence (Fig. 2.46, right). While Fig. 2.45 (right) demonstrates a lack of visual transparency to the interior from outside the building, the views from inside the building adjacent to the facade are largely preserved (Fig. 2.46, left), despite the physical occlusion of over half of the view.

Figure 2.47 shows the automated exterior solar control screens applied as a facade retrofit (revitalisierung) to the Haupthaus KfW building in Frankfurt. In contrast to the previous example, the Haupthaus screens are composed of a glazed sandwich panel with an interlayer of expanded metal. Compared with the previous example, the expanded metal screen results in a significantly lower openness factor at normal incidence (Fig. 2.48, left). However, significant visual information is

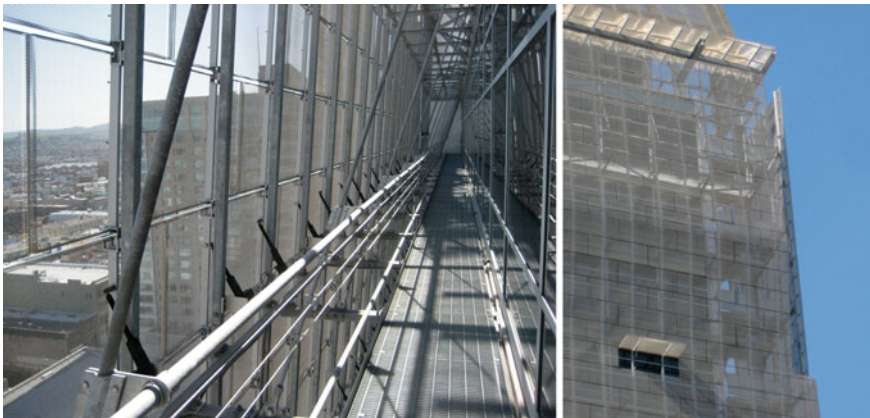


Fig. 2.45 Perforated metal screen used for solar control on the southeast-facing facade of the San Francisco Federal Building. *Note* that the openness factor (50% or 0.5) assumes a view at normal incidence (perpendicular) to the plane of the facade. The *left* image shows how the apparent transparency of the material diminishes significantly for oblique views. The *right* image shows how the exterior screen completely blocks views of the building interior during daylight hours



Fig. 2.46 Interior views looking through the facade glazing and exterior perforated metal screen at distances of 1 m (*left*) and 0.1 m (*right*)



Fig. 2.47 Automated exterior solar control screens applied as a facade retrofit (*revitalisierung*) to the Haupthaus KfW building in Frankfurt (*left*) and interior view with screens deployed (*right*)



Fig. 2.48 The Haupthaus exterior solar control screens are composed of a glazed sandwich panel with an interlayer of expanded metal configured to completely block direct view of the solar disc from the interior while preserving a partial view to the exterior. Images are taken from the building interior at varying distances from the screen (0.2, 1, and 3 m)

preserved, with the content of the window view becoming clearer as the distance of the viewer from the screen increases (Fig. 2.48). In addition, the angular tilt of the expanded metal allows for increasingly open views in a downward direction, enabling views below the horizon to be preserved while increasingly blocking views to the sky that may include the solar disk. Finally, the panels can be completely retracted to enable unobstructed views when solar or glare control is not required.

2.6.6 *Visual Clarity*

In addition to openness factor, the clarity of the window view is an important design consideration for view quality. For example, DIN 5034 makes explicit provisions for the clarity of the view: “For this reason it is necessary to provide windows with transparent, undistorted and neutrally colored glazing at the eye level of persons standing or sitting in a room.” Similarly, LEED (v4) requires that, “view glazing in the contributing area must provide a clear image of the exterior, not obstructed by frits, fibers, patterned glazing, or added tints that distort color balance.” (U.S.G.B.C. 2015). Distortion of the view can result from the application of frit patterns (as shown in Fig. 2.49), prismatic glazing, optical light-redirecting films, or simple light diffusing polymer materials. Tinting or coloration of the view results from alternation of the spectral content of light due to changes made to the chemical formulation of glass to improve solar control and typically produce neutral grey, bronze and blue-green colors.



Fig. 2.49 Horizontal frit pattern applied to portions of the glazed facade of New York Times building

2.6.7 Limitations and Future Directions Related to View

While the parameters outlined in this section present a useful means of evaluating the amount and quality of views during design, it is important to note several limitations with current approaches. First, the view angles calculated during design may omit the presence of interior objects such as furniture and partitions that block direct line of sight for occupants when seated. Second, calculation of direct line-of-sight views and view angles discounts the significant impact of shading devices that are often deployed to address issues related to glare and solar overheating near windows. Figure 2.50 presents an example from the San Francisco Federal Building, contrasting the view content available (left) with the views preserved through the south east facade following the retrofit application of manually operated interior roller shades (openness = 0.03) and a solar control film to address issues related to discomfort glare and occupant solar overheating. This example illustrates the difficulty in preserving quality visual connection to the outdoors, particularly from core zone workstations, without taking an integrated approach to the design of the facade, dynamic shading systems and controls, and the workstations themselves. Third, view factor calculations do not take into consideration the content of the window view, and thus may overestimate the benefit of increased window area near the floor or ceiling that may add little additional visual information of value to occupants. Fourth, quality window views require effective glare control. Therefore, designers may overestimate the value of views that include the path of the sun but do not completely block occupant views of the solar disc, or views with a high level of luminance contrast between the window view and adjacent interior surfaces.

As fenestration systems become more optically complex, the most effective method of differentiating view quality during design will likely be through full-scale physical mockups and human observational studies. Full-scale test facilities such as the LBNL Flexlab (Chap. 4) present an ideal setting for such human factors evaluations, and provide the capability of evaluating human factors outcomes alongside energy and controls optimization objectives. Where physical observation is not practical, such as in the earliest stages of design, simulation

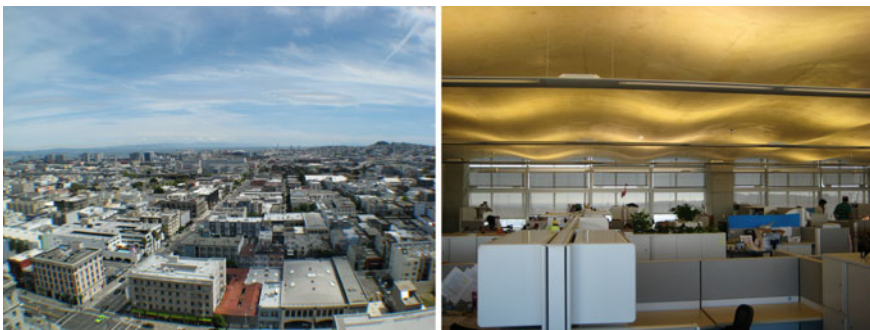


Fig. 2.50 View potential of southeast facing facade (*left*) and actual view from workstation located approximately 10 m (33 ft) from the facade

techniques incorporating image-based lighting (Chap. 3) can serve as a preliminary means of examining simulated views using actual visual context and scene luminances captured from the project site. Finally, as dynamic solar and glare control layers become more common, dynamic view-based metrics will be needed to appropriately differentiate systems based on the fraction of time during occupied hours when quality views are maintained.

Multiple parameters for evaluating the availability, amount, and quality of window views have been presented, including minimum window size, view factor, distance from windows, view content, view occlusion, and view clarity. However, it remains unclear how occupants relatively value trade-offs among these various parameters. To improve the fidelity of design assumptions and occupant satisfaction, it is important to examine buildings in use to assess the applicability of current view-based performance criteria as well as learn how occupants rank the importance of various performance indicators. Similarly, it is important to examine how occupants modify available views to address factors such as privacy and view, visual discomfort and solar control. These issues are discussed in detail in Chap. 6.

2.7 Solar Control and Thermal Comfort

In addition to controlling solar (shortwave) radiation indoors to minimize glare and space cooling loads, exposure to sunlight has a significant impact on occupant thermal comfort.

Because thermal comfort standards were developed assuming occupants would not be directly exposed to shortwave radiation, relevant standards such as ASHRAE Standard 55 (ASHRAE 2004) or ISO Standard 7730 (ISO 2015) do not account for the impacts of shortwave gain on the body of the occupant. Solar radiation falling directly on occupants creates additional, often substantial, thermal stress that is often beyond the capacity of cooling systems to offset. And, because the occurrence of direct sun varies spatially and temporally, systems that attempt to cool sunlit areas often cause thermal discomfort due to overcooling adjacent (non-sunlit) areas. As designers increasingly seek to achieve both daylit and thermally comfortable, energy efficient buildings, the standard design condition for occupant thermal comfort no longer resembles the internal and tightly controlled thermal zones in which existing thermal comfort standards are derived. The critical design condition for assessing thermal comfort in daylit buildings is the daylit perimeter zone (e.g. Figure 2.51), where, until recently, there have been no design tools available to study the effects of solar radiation on indoor thermal comfort.

Figure 2.51 presents an example of direct sun in an unoccupied south-facing perimeter zone workstation on the southeast facade of the San Francisco Federal Building. The image is representative of the original design intent for creating a thermally comfortable daylit perimeter zone through the application of spectrally selective facade glazing (SHGC 0.37) and an exterior solar control screen, with an openness factor of 0.5 at normal incidence. The combined effect of these solar



Fig. 2.51 Unoccupied south-facing perimeter zone workstation on the south-east facade of the San Francisco Federal Building

control layers leads to over an 80% reduction in solar transmission through the facade, and was considered acceptable by the design team for occupant thermal comfort as well as for the level of solar control needed to avoid supplementing the low-energy cooling strategy with an air-conditioning system (McConahey et al. 2002). However, as noted in a post occupancy evaluation of the building, (Konis 2012), the original design was subsequently retrofit with interior shades and a solar control film (solar energy transmission = 0.33) to address issues of occupant solar overheating and visual discomfort.

Recently, Arens et al. (2015) developed *SolarCal*, a model for predicting the effect of indoor solar exposure on occupant thermal comfort. The SolarCal model, “computes an increase in Mean Radiant Temperature (MRT) equivalent to short-wave gains from direct, diffuse and indoor-reflected radiation on a person” (Arens et al., 2015). The solar-adjusted MRT can then be used to compute the Predicted Mean Vote (PMV) using the ASHRAE-55 prescribed method to obtain a more realistic prediction of occupant thermal comfort in spaces with direct sun (Hoyt et al. 2014). Built on the formulae developed for SolarCal, Mackey (2015) developed a solar-adjusted thermal comfort “virtual manikin” integrated within the Ladybug/Honeybee (Sadeghipour 2013) suite of environmental analysis plug-ins for the 3D modeling software Rhinoceros. The thermal manikin software enables designers to compute the thermal sensation that is being experienced by occupants near windows and generate more accurate prediction of thermal comfort.

Figure 2.52 shows the solar adjusted radiant temperature across the surfaces of a thermal comfort manikin during the fall equinox (11:00–12:00). Radiant temperatures on surfaces of the body that exceed typical zone temperatures (e.g. 21–23 °C) indicate the need for additional (often substantial) space cooling and increase the

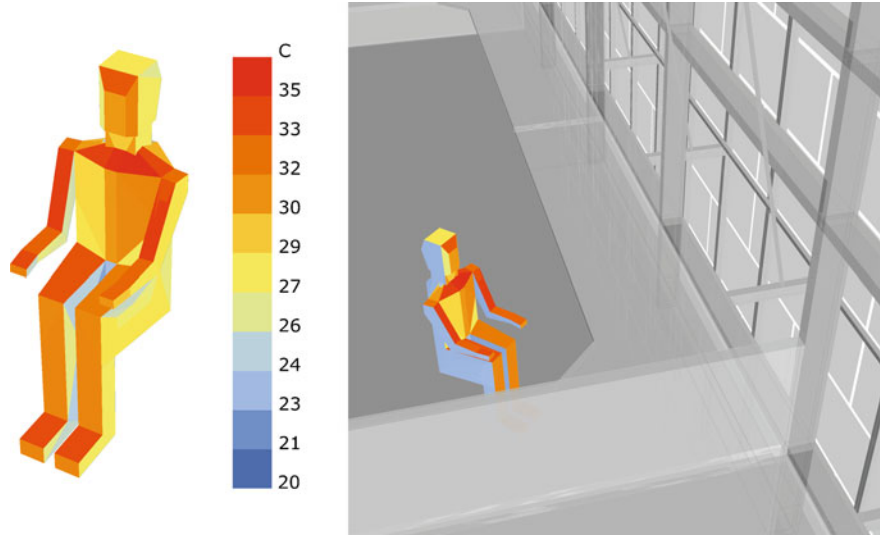


Fig. 2.52 Design condition solar adjusted radiant temperature on thermal comfort manikin (September 21, 11:00–12:00, clear sky conditions, no interior roller shades deployed on the facade)

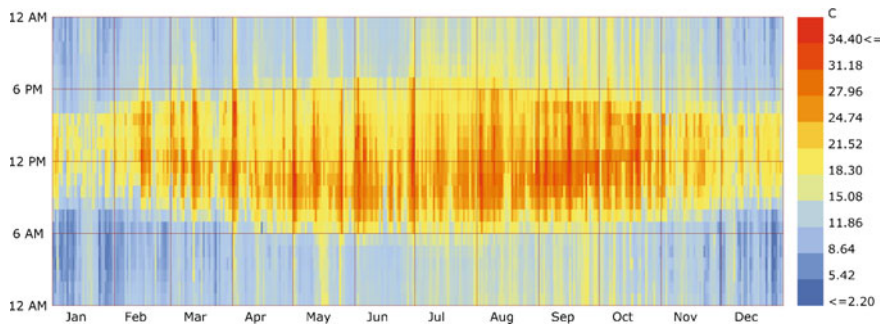


Fig. 2.53 Solar-adjusted MRT on an hourly basis throughout the year

MRT of the occupant relative to an equivalent zone without sun. In the case shown in Fig. 2.52, the resulting solar-adjusted MRT is 35 °C, and the MRT discounting the effects of solar radiation is 19.5 °C. Results can be produced on an hourly basis over an annual period to examine the frequency and magnitude of solar effects on MRT (Fig. 2.53).

Perhaps the greatest benefit for designers is in developing appropriate exterior shading strategies and in selecting material solar optical properties (e.g. glazing SHGC) in response to feedback on occupant solar-adjusted thermal comfort. While effective solar control is needed on an annual basis to avoid occupant modifications or more formal retrofits to the building facade, in early stages of design, a design

condition representing critical solar control requirements can be used. For example, the hours of the year where peak solar-adjusted-MRT occur concurrent with peak outdoor temperatures. While the design team for the San Francisco Federal Building considered occupant thermal comfort in detail during design using the ASHRAE adaptive thermal comfort model (Haves et al. 2004), the resulting fraction of allowed solar transmission can be readily shown to produce thermal discomfort for occupants seated in sunlit areas of the perimeter.

Figure 2.54 shows the design condition solar adjusted radiant temperature on the thermal comfort manikin (September 21, 11:00–12:00, clear sky conditions) for the original (as-built) facade (letter B), the facade following the addition of an interior solar control film (letter C), and a hypothetical scenario with the exterior shading removed from the facade (letter A). Comparison of the various outcomes shows that the removal of the exterior shading would likely lead to extreme thermal discomfort for perimeter zone occupants. It is important to note that this (letter A) is the design condition for most commercial office buildings without external shading, and includes the reduction in solar heat gain provided by high-performance spectrally selective glazing ($SHGC = 0.37$). The retrofit outcome, (letter C), shows that the combined effect of three layers of solar control (exterior, glazing, and film), which achieve a combined SHCG of approximately 0.06 is sufficient to maintain occupant thermal comfort in the perimeter zone.

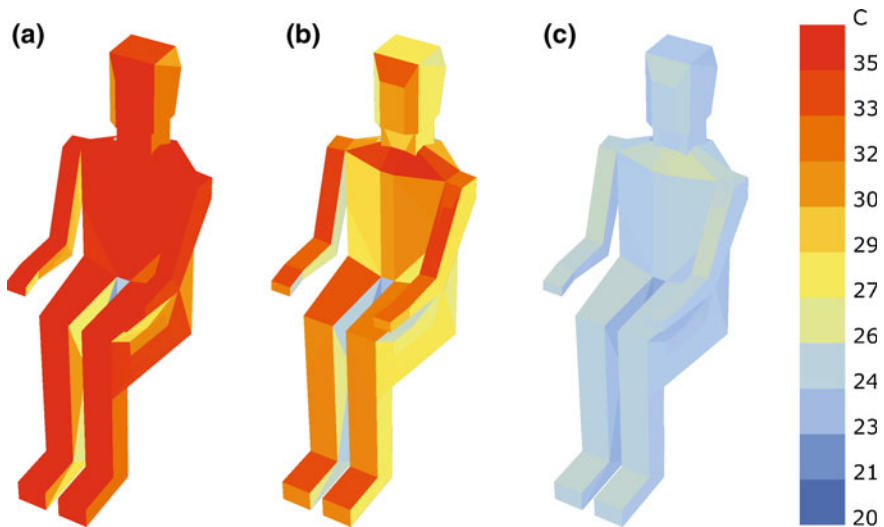


Fig. 2.54 Design condition solar adjusted radiant temperature on thermal comfort manikin for three cases: **a** Facade with exterior shading removed, **b** Facade as designed, **c** Facade with addition of solar control film retrofit (September 21, 11:00–12:00, clear sky conditions)

2.7.1 Limitations and Future Directions of Solar/Thermal Comfort Evaluation

Thoughtful consideration of the impact of shortwave solar radiation on occupant thermal comfort is critical in early stage design to establish a realistic baseline facade configuration for design development including the effects of shading. While dynamic facade systems (discussed in Chap. 3) present a technological approach for more effectively controlling solar exposures in the perimeter zone, it is important to note that the design and operation of automated systems require realistic assumptions for the range of thermal conditions acceptable to occupants. By enabling more realistic predictions of solar-adjusted thermal comfort on an hourly basis, the tools discussed above can be integrated with other annualized simulation approaches to serve as a basis for the operation of automated facade solar control systems that may be designed to dynamically modulate the allowable transmittance of fenestration. The final state of the dynamic facade thus must account for and prioritize the often contradictory requirements of cooling load control, daylight transmittance, glare control, thermal comfort management and view.

2.8 Conclusions

Efforts to achieve daylighting performance goals influence numerous building design parameters with impacts across a range of physical and temporal scales. These include project siting and orientation, form and massing, floor-plate depth, sizing and location of apertures, configuration of fenestration systems, zoning and sizing of mechanical HVAC and lighting systems, interior programming and furnishings, and many other parameters. Energy and occupant performance has one intrinsic time scale, impacts on occupant health and wellbeing may have a longer time frame. Will a building that performs well today also be a top performer in 10 or 20 years? Performance metrics, when integrated into the design process, help to enable a feedback loop to better understand how adjustments to individual parameters (and various combinations of multiple parameters), are likely to affect project performance over these scales. Through iteration, metrics can be used to go beyond compliance-based design outcomes to performance-based design processes that seek the optimum solution among multiple, (and sometimes conflicting) performance objectives. This latter task is dealt with in Chap. 4. Finally, measureable performance goals serve as a basis to compare the performance of the project in use with design intent to inform and refine future design efforts.

References

- Amundadottir et al (2013) Modeling non-visual responses to light: unifying spectral sensitivity and temporal characteristics in a single model structure. In: Proceedings of CIE Centenary Conference “Towards a New Century of Light”, Apr 15–16, 2013, Paris, France, p 101–110
- Amundadottir ML, Lockley SW, Andersen M (2016) Unified framework to evaluate non-visual spectral effectiveness of light for human health. *Lighting Res Technol* 2016:1–24
- Andersen M, Mardaljevic J, Lockley SW (2012) A framework for predicting the non-visual effects of daylight—part I: photobiology-based model. *Lighting Res Technol* 2012(44):37
- Arens E, Hoyt T, Zhou X, Huang L, Zhang H, Schiavon S (2015) Modeling the comfort effects of short-wave solar radiation indoors. *Build Environ* 88:3–9. doi:[10.1016/j.buildenv.2014.09.004](https://doi.org/10.1016/j.buildenv.2014.09.004)
- ASHRAE (2004) ASHRAE. Standard 55-2004: thermal environmental conditions for human occupancy. American society of heating, refrigerating and air-conditioning engineers
- ASHRAE *Performance Measurement Protocols for Commercial Buildings* (PMP) (2010) Atlanta: ASHRAE Inc. http://www.techstreet.com/ashrae/standards/performance-measurement-protocols-for-commercial-buildings?ashrae_auth_token=&gateway_code=ashrae&product_id=1703581
- Bourgeois D, Reinhart CF, Ward G (2008) A standard daylight coefficient model for dynamic daylighting simulations. *Building Res Info* 36(1):68–82
- Brainard GC, Hanifin JP, Greeson JM, Byrne B, Glickman G, Gerner E, Rollag MD (2001) Action spectrum for melatonin regulation in humans: evidence for a novel circadian photoreceptor. *J Neurosci* 21:6405–6412
- Burkhart K, Konis K (2016) Daylighting evaluation of a leed platinum laboratory building: a post-occupancy study comparing performance in use to design intent. PLEA 2016 Los Angeles. Cities, Buildings, People: Towards Regenerative Environments, 11–13 July 2016
- California Energy Commission (CEC) (2003) Windows and offices; A study of office worker performance and the indoor environment. Technical report no. 500-03-082-A-9. <http://www.energy.ca.gov/2003publications/CEC-500-2003-082/CEC-500-2003-082-A-09.PDF>
- California Public Utilities Commission (CPUC) (2008) California long term energy efficiency strategic plan. <http://www.cpuc.ca.gov/general.aspx?id=4125>
- Chang AMM, Scheer FA, Czeisler CA (2011) The human circadian system adapts to prior photic history. *J Physiol* 589(5):1095–1102
- CIE (2004) Ocular lighting effects on human physiology and behavior. Commission Internationale de l’Éclairage Publication 158(2004):2004
- Collins BL (1975) Windows and people: a literature survey. Psychological reaction to environments with and without windows. National Bureau Standards, Washington DC
- DIN 5034 (2011) Tageslicht in Innenräumen, Deutsches Institut für Normung
- École Polytechnique Fédérale de Lausanne (2016) Interdisciplinary Laboratory of Performance-Integrated Design. SpeKtro, Interactive dashboard for exploring non-visual spectrum lighting. <http://spektro.epfl.ch/> Accessed 24 July 2016
- EIA (2012) Commercial building energy consumption survey (CBECS). Table 6. Electricity consumption by end use, 2012
- Einhorn HD (1969) A new method for the assessment of discomfort glare. *Lighting Res Technol* 1(4): 235–247
- Einhorn HD (1979) Discomfort glare: a formula to bridge differences. *Lighting Res Technol* 11(2): 90–94
- Einhorn HD (1998) Unified Glare Rating (UGR): merits and application to multiple sources. *Lighting Res Technol* 30(2):89–93
- Enezi et al (2011) A “melanopic” spectral efficiency function predicts the sensitivity of melanopsin photoreceptors to polychromatic lights. *J Biol Rhythms* 2011(26):314

- Farley KMJ, Veitch JA (2001) A room with a view: a review of the effects of windows on work and well-being. National Research Council of Canada (NRCC) technical report IRC-RR-136. <http://nparc.cisti-icist.nrc-cnrc.gc.ca/eng/view/object/?id=ca18fcef-3ac9-4190-92d9-dc6cbbca7a98>
- Figueiro et al (2016) Designing with circadian stimulus. lighting design and applications (LD + A). The magazine of the Illuminating Engineering Society of North America (IESNA). Published October 2016
- Fry GA, King VM (1975) The pupillary response and discomfort glare. J Illuminating Eng Soc 4 (4) <http://dx.doi.org/10.1080/00994480.1975.10748533>
- Gooley JJ, Lu J, Chou TC, Scammell TE, Saper CB (2001) Melanopsin in cells of origin of the retinohypothalamic tract. Nat Neurosci 4(12):1165
- Hannibal J, Hindersson P, Knudsen SM, Georg B, Fahrenkrug J (2002) The photopigment melanopsin is exclusively present in pituitary adenylate cyclase-activating polypeptide-containing retinal ganglion cells of the retinohypothalamic tract. J Neurosci. 22(1):RC191
- Hattar S, Liao HW, Takao M, Berson DM, Yau KW (2002) Melanopsin-containing retinal ganglion cells: architecture, projections, and intrinsic photosensitivity. Science 295 (5557):1065–1070
- Haves P, Linden PF, Da Graca G Carrilho (2004) Use of simulation in the design of a large, naturally ventilated office building. Building Serv Eng Res Technol 2004(25):211
- Heerwagaen JH, Orians GH (1986) Adaptations to windowlessness: A study of the use of visual décor in windowed and windowless offices. Envir Behav 18(5):623–639
- Heschong L (2012) Heschong Mahone Group. Daylight metrics. California Energy Commission. Publication number: CEC-500-2012-053
- Hopkinson RG, Bradley RC (1960) Glare from very large sources. Illuminating Eng 55:288–297
- Hoyt T, Schiavon S, Piccioli A, Moon D, Steinfeld K (2014) CBE thermal comfort tool. Berkeley: Center for the Built Environment, University of California 2012e2014. <http://smap.cbe.berkeley.edu/comforttool/> last Accessed 20 June 14
- Huang J, Franconi E (1999) Commercial heating and cooling loads component loadanalysis. Building technologies department, Lawrence Berkeley National Laboratory; 1999. LBNL-37208
- IEA SHC Task 21 (2000) Daylight in buildings. A source book on daylightingsystems and components. A report of IEA SHC Task 21/ ECBCS Annex 29, July 2000. <https://buildings.lbl.gov/sites/all/files/daylight-in-buildings.pdf>
- IESNA (2016) Lighting handbook. In: DiLaura D, Houser K, Mistrick R, Steffy G (eds) ISBN # 978-0-87995-241-9
- Illuminating Engineering Society of North America. Approved Method: IES Spatial Daylight Autonomy (sDA) and Annual Sunlight Exposure (ASE) (2012) IES LM-83-12
- Inanici M, Brennan M, Clark E (2015). Multi-spectral Lighting Simulations: computing circadian light. International Building Performance Simulation Association (IBPSA) 2015 Conference, Hyderabad, India, December 7–9, 2015
- International Well Building Institute (2016) WELL Building Standard (v1). May 2016
- ISO 7730 (2005). Ergonomics of the thermal environment analytical determination and interpretation of thermal comfort using calculation of the PMV and PPD indices and local thermal comfort criteria. 3rd version. Geneva: International Organization for Standardization; 2005
- Jakubiec JA, Reinhart CF (2011) DIVA 2.0: Integrating Daylighting And Thermal Simulations Using Rhinoceros 3D, DAYSIM and EnergyPlus. In: Proceedings of building simulation 2011:12th conference of international building performance simulation association, Sydney, 14–16 November
- Jakubiec JA, Reinhart CF (2012) The ‘adaptive zone’—A concept for assessing discomfort glare throughout daylight spaces.” Lighting Res Technol 44(2): 149–70, Originally published online October, 2011
- Jakubiec JA, Reinhart CF, Van Den Wymelenberg K (2016) Towards an integrated framework for predicting visual comfort conditions from luminance-based metrics in perimeter daylight spaces. In: Proceedings of bs2015: 14th conference of international building performance simulation association, Hyderabad, India, Dec. 7–9, 2015

- Kaplan R (1993) The role of nature in the context of the workplace. *Landscape Urban Planning* 26:193–201
- Kellert Heerwagen (2008). *Biophilic design: the theory, science and practice of bringing buildings to life*. p 432. Wiley. ISBN: 978-0-470-16334-4
- Khalsa SBS, Jewett ME, Cajochen C, Czeisler CA (2003) A phase response curve to single bright light pulses in human subjects. *J Physiol* 15:945–952
- Klepeis NE, Nelson WC, Ott WR, Robinson J, Tsang AM, Switzer P, Behar JV, Hern S, Engelmann W (2001) The national human activity pattern survey (NHAPS): a resource for assessing exposure to environmental pollutants. *J Expos Analysis Environ Epidemiol* 11(3): 231–252
- Konis K (2012) A method for measurement of transient discomfort glare conditions and occupant shade control behavior in the field using low-cost CCD cameras. American solar energy society (ASES) National solar conference, Denver, Colorado, May
- Konis K (2016) A novel circadian daylight metric for building design and evaluation. *building and environment*, Vol 113, 15 February 2017, Pages 22–38 <http://www.sciencedirect.com/science/article/pii/S0360132316304498> <http://dx.doi.org/10.1016/j.buildenv.2016.11.025>
- Lam WMC (1977) *Perception and lighting as formgivers for architecture*. McGraw-Hill, Inc Lark Spectral Lighting. http://faculty.washington.edu/inanici/Lark/Lark_home_page.html Accessed 25 July 2016
- Lighting Research Center (2016) Circadian stimulus calculator. <http://www.lrc.rpi.edu/programs/lightHealth/> Accessed 8 June 2016
- Lockley SW, Brainard GC, Czeisler CA. (2003) High sensitivity of the human circadian melatonin rhythm to resetting by short wavelength light *J Clin Endocrinol Metab* 88(9):4502–4505
- Lucas RJ, Peirson SN, Berson DM, Brown TM, Cooper HM et al (2014) Measuring and using light in the melanopsin age. *Trends Neurosci* 31(1):1–9
- Lucas et al (2016) Excel-based melanopic illuminance calculator. <http://lucasgroup.lab.is.manchester.ac.uk/research/measuringmelanopicilluminance/> Accessed 25 July 2016
- Lyness JA (1977) Discomfort glare and visual distraction. *Light Res Technol* 9:51–52
- Mackey C (2015) *Pan climatic humans: shaping thermal habits in an unconditioned society*. Thesis: M. Arch., Massachusetts Institute of Technology, Department of Architecture, 2015. <http://hdl.handle.net/1721.1/99261>
- Mardaljevic J (2006) CIBSE national conference 2006: engineering the future. 21–22 March 2006, Oval Cricket Ground, London, UK
- McConahey E, Haves P, Chirst T (2002) The integration of engineering and architecture: a perspective on natural ventilation for the new san francisco federal building In: 2002 ACEEE summer study on energy efficiency in buildings. Asilomar, California, USA, 2002. <https://eetd.lbl.gov/sites/all/files/publications/lbnl-51134.pdf>
- Moon P, Spencer DE (1942) *Illumination from a non-uniform sky*. Illum, Eng
- Nabil A, Mardaljevic J (2005) Useful daylight illuminance: a new paradigm to access daylight in buildings. *Ligh Res Technol* 37(1):41–59
- Ne’eman E, Hopkinson RG (1970) Critical minimum acceptable window size: A study of window design and provision of a view. *Light Res Technol* 2:17–27
- Peña R (2014) Living proof. The Bullitt Center, High performance building case study. <http://neea.org/docs/default-source/default-document-library/living-proof—bullitt-center-case-study.pdf?sfvrsn=6>
- Phipps-Nelson J, Redman JR, Dijk D-JJ, Rajaratnam SM (2003) Daytime exposure to bright light, as compared to dim light, decreases sleepiness and improves psychomotor vigilance performance. *Sleep* 26(6):695–700
- Provencio I, Rodriguez IR, Jiang G, Hayes WP, Moreira EF, Rollag MD (2000) A novel human opsin in the inner retina. *J Neurosci* 20(2):600–605
- Rea and Bierman (2016) A new rationale for setting light source luminous efficacy requirements. *Light Res Technol* September 10, 2016 doi:[10.1177/1477153516668230](https://doi.org/10.1177/1477153516668230)
- Rea MS et al (2012) Modelling the spectral sensitivity of the human circadian system. *Ligh Res Technol* 44(4):386–396

- Reinhart CF (2002) Lightswitch 2002: a model for manual control of electric lighting and blinds. *Solar Ener* 77(1): 15–28 doi:[10.1016/j.solener.2004.04.003](https://doi.org/10.1016/j.solener.2004.04.003)
- Reinhart C (2015) Opinion: Climate-based daylighting metrics in LEEDv4-A fragile progress. *Light Res Technol* 47(4):388
- Reinhart CF, Herkel S (2000) The simulation of annual daylight illuminance distributions—a state of the art comparison of six RADIANCE based methods. *Energy Build* 32(2):167–187. doi:[10.1016/S0378-7788\(00\)00042-6](https://doi.org/10.1016/S0378-7788(00)00042-6)
- Rogers Z (2006) Daylighting metric development using daylight autonomy calculations in the sensor placement optimization tool. Boulder, Colorado, USA: Architectural Energy Corporation. https://www.daylightinginnovations.com/system/public_assets/original/SPOT_Daylight%20Autonomy%20Report.pdf
- Ruuger M, Gordijn MCM, Beersma DGM, de Vries B, Daan S (2006) Time-of-day-dependent effects of bright light exposure on human psychophysiology: comparison of daytime and nighttime exposure. *Am J Physiol-Reg I* 290(5)
- Sadeghipour R, Mostapha PM (2013) Ladybug: a parametric environmental plugin for grasshopper to help designers create an environmentally-conscious design. In: Proceedings of the 13th International IBPSA Conference Held in Lyon, France Aug 25–30th. http://www.ibpsa.org/proceedings/BS2013/p_2499.pdf
- Selkowitz SE, Kim J-J, Navvab M, Winkelmann FC (1982) The DOE-2 and superlite daylighting programs. LBNL report number LBL-14569. <https://eetd.lbl.gov/node/50815>
- Shehabi A, DeForest N, McNeil A, Masanet E, Lee ES, Milliron D (2013) US energy savings potential from dynamic daylighting control glazings. *Energy Build* 66(2013):415–423
- Suk JY, Schiler M, Kensek K (2013) Development of new daylight glare analysis methodology using absolute glare factor and relative glare factor. *Energy Buildings* 64:113–122
- Suk Jae, Schiler M, Kensek K (2016) Absolute glare factor and relative glare factor based metric: predicting and quantifying levels of daylight glare in office space. *Energy Build* 130(15):8–19
- Thapan K, Arendt J, Skene DJ (2001) An action spectrum for melatonin suppression: evidence for a novel non-rod, non-cone photoreceptor system in humans. *J Physiol* 535:261–267
- Torcellini P et al (2006) Lessons learned from field evaluation of six high-performance buildings. NREL/CP-550-36290
- Tregenza PR, Waters IM (1983) Daylight coefficients. *Light Res Technol* 15(2):65–71. doi:[10.1177/096032718301500201](https://doi.org/10.1177/096032718301500201)
- Tuaycharoen N, Tregenza PR (2007) View and discomfort glare from windows. *Light Res Technol* 39(2):185–200
- Ulrich RS, Simons RF, Losito BD, Fiorito E, Miles MA, Zelson M (1991) Stress recovery during exposure to natural and urban environments. *J Environ Psychol* 11(3):201–230
- U.S. Green Building Council (2009). LEED 2009 for new construction and major renovations. Reference guide
- U.S. Department of Energy (DOE) (2015). A common definition for zero energy buildings. http://energy.gov/sites/prod/files/2015/09/f26/bto_common_definition_zero_energy_buildings_093015.pdf
- U.S. Green Building Council. (2016). LEED v4 for building design and construction. April 5, 2016. 161 pages. http://in.usgbc.org/sites/default/files/LEED%20v4%20BDC_04.05.16_current.pdf
- Van Den Wymelenberg KG (2012) Evaluating human visual preference and performance in an office environment using luminance-based metrics. PhD Dissertation, University of Washington. ProQuest, LLC
- Van Den Wymelenberg K, Inanici MN (2014) A critical investigation of common lighting design metrics for predicting human visual comfort in offices with daylight. *LEUKOS* 10(3):145–164
- Veitch JA, Farley KMJ (2001) A room with a view: a review of the effects of windows on work and well-being. National Research Council of Canada (NRCC) technical report IRC-RR-136. <http://nparc.cisti-icist.nrccnrc.gc.ca/eng/view/object/?id=ca18fccf-3ac9-4190-92d9-dc6cbbca7a98>
- Vos JJ (1984) Disability glare—a state of the art report. *CIE J.* 3:39–53

- Ward G (1992) RADIANCE visual comfort calculation. <http://radsite.lbl.gov/radiance/refer/Notes/glare.html>
- Ward GL, Shakespeare R (1998) Rendering with radiance. Morgan Kaufmann, 1998. ISBN 1-55860-499-5
- Weinold J (2009) Dynamic daylight glare evaluation. building simulation. Eleventh International IBPSA Conference. Glasgow Scotland, July 27–30, 2009. http://www.ibpsa.org/proceedings/BS2009/BS09_0944_951.pdf
- Wienold J, Christoffersen J (2006) Evaluation methods and development of a new glare prediction model for daylight environments with the use of CCD cameras. Energy Build 38(7):743–757
- Wilson EO (1993) Biophilia. Harvard University Press, ISBN 9780674074422
- Zelinski EL, Deibel SH, McDonald RJ (2014) The trouble with circadian clock dysfunction: multiple deleterious effects on the brain and body. Neurosci Biobehavioral Rev 40:80–101

<http://www.springer.com/978-3-319-39461-9>

Effective Daylighting with High-Performance Facades

Emerging Design Practices

Konis, K.; Selkowitz, S.

2017, XVI, 269 p. 233 illus., 183 illus. in color.,

Hardcover

ISBN: 978-3-319-39461-9